

Sparse Logistic Tensor Decomposition for Binary Data

Jianhao Zhang and Yoonkyung Lee

Department of Statistics, The Ohio State University

Abstract

Tensor data are increasingly available in many application domains. We develop several tensor decomposition methods for binary tensor data. Different from classical tensor decompositions for continuous-valued data with squared error loss, we formulate logistic tensor decompositions for binary data with a Bernoulli likelihood. To enhance the interpretability of estimated factors and improve their stability further, we propose sparse formulations of logistic tensor decomposition by considering ℓ_1 -norm and ℓ_0 -norm regularized likelihood. To handle the resulting optimization problems, we develop computational algorithms which combine the strengths of tensor power method and majorization-minimization (MM) algorithm. Through simulation studies, we demonstrate the utility of our methods in analysis of binary tensor data. To illustrate the effectiveness of the proposed methods, we analyze a dataset concerning nations and their political relations and perform co-clustering of estimated factors to find associations between the nations and political relations.

Keywords: Binary data, Majorization-Minimization algorithm, Sparsity, Tensor decomposition

1 Introduction

As a natural generalization of vectors and matrices, tensors have appeared frequently as a data form in many fields including social networks (Nickel et al., 2011), recommender systems (Bi et al., 2018) and genomics (Wang et al., 2019). As a result, tensor decomposition has attracted interests from machine learning and statistics with applications in chemometrics (Bro, 1997), computer vision and signal processing. See Kolda and Bader (2009) for a comprehensive review. In general, there are two approaches to decomposition of tensor data: CP decomposition and Tucker decomposition. CP decomposition is the abbreviation of canonical decomposition (CANDECOMP) and parallel factor (PARAFAC) analysis, which were proposed independently in psychometrics by Harshman (1970) and Carroll and Chang (1970). Tucker decomposition (Tucker, 1966) is a generalization of singular value decomposition for higher-order data, which includes CP decomposition as a special case.

There has been a growing body of literature that extends tensor decomposition methods for real valued data to other types such as tensors with binary outcomes or counts for dimensionality reduction and latent factor modeling. As a closely related problem, various types of principal component analysis (PCA) and matrix factorization methods have been developed for discrete non-Gaussian matrix data (Collins et al., 2002; de Leeuw, 2006; Udell et al., 2016; Landgraf and Lee, 2020b,a). Extending the matrix factorization approach in Collins et al. (2002) to binary tensor

data, Mažgut et al. (2014) considered a Tucker decomposition of the logit parameter tensor, and Wang and Li (2020) considered a CP decomposition of the logit parameter tensor with max-norm constraint and investigated its statistical optimality. More generally, Hong et al. (2020) proposed a CP decomposition of the natural parameter tensor for exponential family data.

In this paper, we focus on binary tensor data and consider settings where sparse latent factors are desired for modeling the underlying logit parameter tensor. Taking collaborative filtering as an example, how users interact with items in different contexts can be organized in the form of a tensor with user, item and context as three modes. Presence or absence of a user’s interaction with an item in each context then makes up a binary tensor. Relations between the users and items could be context-specific, and they may involve a small subset of users, items, or contexts, rendering such relational factors sparse. Benefits of sparse factors and principal components for high dimensional matrix data have been well understood. Similar to sparse PCA (Jolliffe et al., 2003; Zou et al., 2006; Shen and Huang, 2008), sparsity or regularization of factors is often desired in tensor decompositions. Sparsity in estimated factor matrices can provide a concise description of the latent structure and improved understanding of the latent factors in relation to the observable features. For real valued tensors, Allen (2012) and Sun et al. (2017) proposed sparse tensor decomposition methods based on the CP decomposition with an ℓ_1 -norm penalty and ℓ_0 -norm constraint on factor matrices, respectively. Besides, Madrid-Padilla and Scott (2017) considered sparse tensor decomposition with generalized lasso penalties on factor matrices to obtain smoothly varying factors. Zhang and Han (2019) proposed a sparse tensor singular value decomposition based on the Tucker decomposition and studied its statistical optimality.

To handle binary tensor data efficiently, we combine dimensionality reduction with regularization and selection of features and consider sparse decomposition of a logit parameter tensor. We propose a formulation of sparse logistic tensor decomposition by imposing an ℓ_1 -norm penalty or ℓ_0 -norm constraint on the factor matrices in the CP decomposition of a centered logit parameter tensor. Our approach naturally extends the sparse tensor decomposition (Allen, 2012; Sun et al., 2017) to binary data and also extends the sparse logistic PCA (Lee et al., 2010b; Lee and Huang, 2014) to higher-order data.

Rank-one components in the decomposition of the underlying logit tensor generally correspond to multiplicative interactions among different modes. For this reason, sparse factors are well suited for modeling more local patterns of interactions involving only a subset of features along each mode. Such patterns can reveal interesting co-clustering structures between different modes. For binary matrices, Lee and Huang (2014) demonstrated the idea of co-clustering with a biclustering algorithm. Recently, Li (2020) proposed a more general co-clustering analysis framework for exponential family tensor data.

Computationally, binary tensor decomposition entails maximization of the likelihood of a logit parameter tensor under a Bernoulli distribution assumption on the binary entries. Incorporating an ℓ_1 -norm penalty or ℓ_0 -norm constraint on the factors in the decomposition for encouraging sparsity leads to regularization of the likelihood. To solve the resulting optimization problems, we develop several novel computational algorithms. In a nutshell, we combine the strengths of tensor power method for tensor decompositions and majorization-minimization (MM) algorithms, which have been successfully applied in logistic PCA and exponential family PCA for matrix data. By majorizing the negative log likelihood with a quadratic function, we turn the logistic CP decomposition problems with binary data into iterative applications of a plain CP decomposition with real-valued data. Thereby, we could make use of the tensor power method and its adaptations to sparse tensor decompositions for analysis of binary data. In particular, we adopt the tensor power method with alternating rank-one updates (Anandkumar et al., 2014) in the MM approach to logistic tensor decomposition. Further, we incorporate the truncated power method (Yuan and

Zhang, 2013; Sun et al., 2017) for the ℓ_0 -norm constrained logistic tensor decomposition and the soft-thresholding power method (Witten et al., 2009; Allen, 2012) for the ℓ_1 -norm penalized logistic tensor decomposition. We illustrate the utility of the proposed algorithms for analysis of binary tensor data.

The rest of the paper is organized as follows. Section 2 reviews tensor decomposition for real-valued tensor data. In Section 3, we introduce logistic CP decomposition for binary data using a Bernoulli likelihood and present sparse logistic CP decomposition using a regularized likelihood in Section 4. In addition, Sections 3 and 4 include MM-based computational algorithms for logistic tensor decomposition and sparse counterpart, respectively. Section 5 regards an extension of logistic CP decomposition for handling missing data and tensor completion. In Section 6, we discuss several criteria for choosing the rank of tensor decomposition and tuning parameters. We present simulation studies in Section 7 and demonstrate the effectiveness of sparse logistic CP decomposition with an application to nations data in Section 8. We summarize our contributions and list several directions for further investigation in Section 9.

2 Preliminaries

This section provides a technical background of tensor decomposition. Throughout the paper we focus on third-order tensor data, which are common in many applications. Methods for higher-order tensors can be developed similarly.

2.1 Notation

For $p \in \mathbb{N}$, we use $[p]$ to denote the index set $\{1, \dots, p\}$. For two tensors \mathcal{X} and $\mathcal{Y} \in \mathbb{R}^{p_1 \times p_2 \times p_3}$, the inner product of \mathcal{X} and \mathcal{Y} is defined as $\langle \mathcal{X}, \mathcal{Y} \rangle = \sum_{\omega \in [p_1] \times [p_2] \times [p_3]} \mathcal{X}(\omega) \mathcal{Y}(\omega)$. This induces the Frobenius norm of \mathcal{X} as $\|\mathcal{X}\|_F = \sqrt{\langle \mathcal{X}, \mathcal{X} \rangle}$, similar to the Frobenius norm of a matrix.

A tensor can be transformed into a matrix or *matricized* by unfolding it in a given mode. The mode- n matricization of a tensor $\mathcal{X} \in \mathbb{R}^{p_1 \times p_2 \times p_3}$ is denoted by $X_{(n)}$ for $n \in [3]$. For example, $X_{(1)} \in \mathbb{R}^{p_1 \times p_{-1}}$ with $p_{-1} = p_2 p_3$ is a matrix whose columns are the mode-1 fibers of \mathcal{X} . Multiplication of a tensor by a matrix in mode n is called the mode- n matrix product and denoted by \times_n . For example, the mode-1 matrix product of a tensor $\mathcal{X} \in \mathbb{R}^{p_1 \times p_2 \times p_3}$ and a matrix $U \in \mathbb{R}^{q \times p_1}$ is denoted by $\mathcal{X} \times_1 U \in \mathbb{R}^{q \times p_2 \times p_3}$.

The outer product of vectors $\mathbf{a} \in \mathbb{R}^I$ and $\mathbf{b} \in \mathbb{R}^J$ is denoted by $\mathbf{a} \circ \mathbf{b} \in \mathbb{R}^{I \times J}$. For a vector $\mathbf{v} \in \mathbb{R}^p$, $\|\mathbf{v}\|_2$ refers to the Euclidean norm, $\|\mathbf{v}\|_1$ the ℓ_1 -norm, and $\|\mathbf{v}\|_0$ the number of non-zero entries in \mathbf{v} . The Kronecker product of matrices $A \in \mathbb{R}^{I \times J}$ and $B \in \mathbb{R}^{K \times L}$ is denoted by $A \otimes B \in \mathbb{R}^{IK \times JL}$ with $a_{ij}B$ in the ij th block. The Khatri-Rao product of matrices $A \in \mathbb{R}^{I \times K}$ and $B \in \mathbb{R}^{J \times K}$ is the columnwise Kronecker product of A and B denoted by $A \odot B = [\mathbf{a}_1 \otimes \mathbf{b}_1 \ \mathbf{a}_2 \otimes \mathbf{b}_2 \ \dots \ \mathbf{a}_K \otimes \mathbf{b}_K] \in \mathbb{R}^{IJ \times K}$. The Hadamard product of matrices $A \in \mathbb{R}^{I \times J}$ and $B \in \mathbb{R}^{I \times J}$ is the elementwise product of A and B denoted by $A * B = [a_{ij}b_{ij}] \in \mathbb{R}^{I \times J}$. The Hadamard product of two tensors can be defined analogously.

The following property of the Kronecker product will be useful. Let $\mathcal{X} \in \mathbb{R}^{p_1 \times p_2 \times \dots \times p_N}$ and $A^{(n)} \in \mathbb{R}^{q_n \times p_n}$ for each $n \in [N]$. Then $\mathcal{Y} = \mathcal{X} \times_1 A^{(1)} \times_2 A^{(2)} \dots \times_N A^{(N)}$ is equivalent to $Y_{(n)} = A^{(n)} X_{(n)} (A^{(N)} \otimes \dots \otimes A^{(n+1)} \otimes A^{(n-1)} \dots \otimes A^{(1)})^T$ for every $n \in [N]$.

2.2 Tensor Decomposition

We briefly review tensor decomposition for real-valued tensor data. The idea of a CP decomposition (Carroll and Chang, 1970; Harshman, 1970) is to factorize a tensor $\mathcal{X} \in \mathbb{R}^{p_1 \times p_2 \times p_3}$ into a

sum of rank-one component tensors of the form:

$$\mathcal{X} \approx \sum_{r \in [R]} d_r \cdot \mathbf{u}_r \circ \mathbf{v}_r \circ \mathbf{w}_r,$$

where $\mathbf{u}_r \in \mathbb{R}^{p_1}$, $\mathbf{v}_r \in \mathbb{R}^{p_2}$, $\mathbf{w}_r \in \mathbb{R}^{p_3}$, $d_{\max} = d_1 \geq \dots \geq d_R = d_{\min} > 0$, and $\mathbf{u}_r^T \mathbf{u}_r = 1$, $\mathbf{v}_r^T \mathbf{v}_r = 1$, $\mathbf{w}_r^T \mathbf{w}_r = 1$ for $r \in [R]$. Here R is the rank of the tensor \mathcal{X} . This can be formulated as a minimization problem with squared error loss:

$$\min_{\mathbf{d}, U, V, W} \|\mathcal{X} - \sum_{r \in [R]} d_r \cdot \mathbf{u}_r \circ \mathbf{v}_r \circ \mathbf{w}_r\|_F^2,$$

where $\mathbf{d} = (d_1, \dots, d_R)^T \in \mathbb{R}^R$ is a vector of weight parameters, and $U = [\mathbf{u}_1, \dots, \mathbf{u}_R] = [u_{ir}] \in \mathbb{R}^{p_1 \times R}$, $V = [\mathbf{v}_1, \dots, \mathbf{v}_R] = [v_{jr}] \in \mathbb{R}^{p_2 \times R}$, and $W = [\mathbf{w}_1, \dots, \mathbf{w}_R] = [w_{kr}] \in \mathbb{R}^{p_3 \times R}$ are the factor matrices. It's worth noting that this CP decomposition has the property of essential uniqueness. That is, the columns of U, V and W are determined up to joint permutation.

Kruskal (1977, 1989) provided a sufficient condition for the uniqueness of a three-way CP decomposition up to permutation and rescaling of rank-one tensors. Kruskal's condition is

$$k_U + k_V + k_W \geq 2R + 2,$$

where k_U, k_V and k_W are the Kruskal ranks of the matrices U, V and W .

The Tucker decomposition (Tucker, 1966) aims at approximating a tensor $\mathcal{X} \in \mathbb{R}^{p_1 \times p_2 \times p_3}$ with a reduced core tensor $\mathcal{S} \in \mathbb{R}^{R_1 \times R_2 \times R_3}$ and factor matrices $U \in \mathbb{R}^{p_1 \times R_1}$, $V \in \mathbb{R}^{p_2 \times R_2}$, and $W \in \mathbb{R}^{p_3 \times R_3}$ as follows:

$$\mathcal{X} \approx \mathcal{S} \times_1 U \times_2 V \times_3 W.$$

Again this can be formulated as an optimization problem with squared error loss:

$$\min_{\mathcal{S}, U, V, W} \|\mathcal{X} - \mathcal{S} \times_1 U \times_2 V \times_3 W\|_F^2,$$

where $U^T U = I_{R_1}$, $V^T V = I_{R_2}$, and $W^T W = I_{R_3}$. Here R_1, R_2 and R_3 are the numbers of components in the factor matrices U, V and W , respectively. The CP decomposition can be viewed as a special case of the Tucker decomposition when the core tensor \mathcal{S} is super-diagonal and $R_1 = R_2 = R_3 = R$. However, the Tucker decomposition doesn't have uniqueness since we can multiply factor matrices by nonsingular matrices and define a new core tensor and new factor matrices.

A comprehensive review of tensor decomposition is available in Kolda and Bader (2009). In this paper, we focus on the CP decomposition for tensors as it is a more natural choice for defining latent factors, and it is also more amenable to computation. The use of squared error loss can be regarded as an implicit normal distribution assumption for real-valued tensor data. We will employ an alternative loss for binary tensor data.

3 CP Decomposition for Binary Data

3.1 Logistic CP Decomposition

To handle tensors with dichotomous outcomes in many applications, we consider a binary tensor $\mathcal{X} = (x_{ijk}) \in \{0, 1\}^{p_1 \times p_2 \times p_3}$, where each entry x_{ijk} encodes one of the two types of outcomes (e.g., absence or presence) with 0 or 1. We posit a generative model for the tensor and assume that

x_{ijk} are realizations of mutually independent Bernoulli random variables with probability p_{ijk} , or $x_{ijk} \sim \text{Bernoulli}(p_{ijk})$.

For a Bernoulli random variable with probability parameter p , the probability mass function is $P(X = x) = p^x(1-p)^{1-x}$, and $\log P(X = x) = x \log \frac{p}{1-p} + \log(1-p)$. Reparametrizing with the logit parameter $\theta := \log \frac{p}{1-p}$, the log likelihood of θ based on x is given by $\ell(x; \theta) = x\theta - \log(1 + \exp(\theta))$.

Letting $\theta_{ijk} := \log \frac{p_{ijk}}{1-p_{ijk}}$ for individual data entries x_{ijk} in the binary tensor \mathcal{X} , we derive the log likelihood of the logit parameter tensor $\Theta = (\theta_{ijk}) \in \mathbb{R}^{p_1 \times p_2 \times p_3}$ as follows:

$$\begin{aligned} \ell(\mathcal{X}; \Theta) &= \sum_{i,j,k} \{x_{ijk}\theta_{ijk} - \log(1 + \exp(\theta_{ijk}))\} \\ &= \langle \mathcal{X}, \Theta \rangle - \langle \mathbf{1}_{p_1 p_2 p_3}, \log(\mathbf{1}_{p_1 p_2 p_3} + \exp(\Theta)) \rangle, \end{aligned}$$

where $\mathbf{1}_{p_1 p_2 p_3} := \mathbf{1}_{p_1} \circ \mathbf{1}_{p_2} \circ \mathbf{1}_{p_3} \in \mathbb{R}^{p_1 \times p_2 \times p_3}$ is the tensor with all entries equal to one, and $\log(\cdot)$ and $\exp(\cdot)$ are taken as element-wise operators with tensors. Naturally extending the exponential family PCA for a data matrix in Collins et al. (2002) to a higher-order tensor, we consider a CP decomposition of the logit parameter tensor Θ rather than the binary data tensor \mathcal{X} itself and call it *logistic tensor decomposition*.

We include an offset term $\mu \in \mathbb{R}$ in logistic CP decomposition taken as an overall logit parameter value and consider the following decomposition:

$$\Theta = \mu \mathbf{1}_{p_1 p_2 p_3} + \sum_{r \in [R]} d_r \cdot \mathbf{u}_r \circ \mathbf{v}_r \circ \mathbf{w}_r \quad (1)$$

or $\theta_{ijk} = \mu + \sum_{r \in [R]} d_r u_{ir} v_{jr} w_{kr}$, where the multiplicative part has rank R . Standard logistic CP decomposition in the literature assumes $\mu = 0$. For notational convenience, we use Θ_c to refer to $\sum_{r \in [R]} d_r \cdot \mathbf{u}_r \circ \mathbf{v}_r \circ \mathbf{w}_r$, the portion of Θ adjusted by the offset.

To find a CP decomposition of Θ of rank R given the binary tensor \mathcal{X} , we maximize the log likelihood or equivalently minimize the negative log likelihood and formulate a *logistic CP decomposition* problem as follows:

$$\begin{aligned} \min_{\mu, \mathbf{d}, U, V, W} \quad & - \langle \mathcal{X}, \Theta \rangle + \langle \mathbf{1}_{p_1 p_2 p_3}, \log(\mathbf{1}_{p_1 p_2 p_3} + \exp(\Theta)) \rangle \\ \text{s.t.} \quad & \Theta = \mu \mathbf{1}_{p_1 p_2 p_3} + \sum_{r \in [R]} d_r \cdot \mathbf{u}_r \circ \mathbf{v}_r \circ \mathbf{w}_r, \\ & \mathbf{u}_r^T \mathbf{u}_r = 1, \mathbf{v}_r^T \mathbf{v}_r = 1, \mathbf{w}_r^T \mathbf{w}_r = 1, \text{ and } d_r > 0 \text{ for } r \in [R], \end{aligned} \quad (2)$$

where $\mathbf{d} \in \mathbb{R}^r$, $U \in \mathbb{R}^{p_1 \times R}$, $V \in \mathbb{R}^{p_2 \times R}$ and $W \in \mathbb{R}^{p_3 \times R}$ are the weight vector and factor matrices as defined before. While the objective function in (2), $-\ell(\mathcal{X}; \Theta)$, is convex in Θ , it is not convex in the factor matrices jointly, and this leads to a non-convex optimization problem with possibly multiple local optima. Further, the objective function in (2) is convex in each factor when the other two factors are fixed, but the unit norm constraint on each factor makes the problem non-convex.

3.2 Majorization-Minimization Approach

For logistic PCA and exponential family PCA involving similar optimization problems, Majorization-Minimization (MM) algorithms (Hunter and Lange, 2004) have been used successfully. See de Leeuw (2006); Lee et al. (2010b); Lee and Huang (2014); Landgraf and Lee (2020b) for example. To solve the logistic CP decomposition problem in (2), we propose to majorize the objective function with a quadratic loss function and apply state-of-the-art algorithms for CP decomposition iteratively.

To majorize the negative likelihood, we first rewrite $P(X = x) = p^x(1 - p)^{1-x} = \sigma(q\theta)$ with the sigmoid function $\sigma(x) = \text{logit}^{-1}(x) = \{1 + \exp(-x)\}^{-1}$ and $q = 2x - 1$, and use the following tight and uniform quadratic majorization of $-\log \sigma(x)$ from Jaakkola and Jordan (2000); de Leeuw (2006):

$$\begin{aligned} -\log \sigma(x) &\leq -\log \sigma(y) + (\sigma(y) - 1)(x - y) + \frac{2\sigma(y) - 1}{4y}(x - y)^2 \\ &\leq -\log \sigma(y) + (\sigma(y) - 1)(x - y) + \frac{1}{8}(x - y)^2, \end{aligned}$$

where the equalities hold when $x = y$. We will focus on the uniform bound (the second inequality) for computational convenience and leave the tight bound (the first inequality) for future study.

Let $\Theta^{[m]}$ be the estimate of Θ obtained in the m th step of the MM algorithm. Then, applying the above majorization to $-\log \sigma(q_{ijk}\theta_{ijk})$ at $\theta_{ijk}^{[m]}$ with $q_{ijk} = 2x_{ijk} - 1$ and completing the square, we have

$$-\ell(\mathcal{X}; \Theta) = -\sum_{i,j,k} \log \sigma(q_{ijk}\theta_{ijk}) \leq -\sum_{i,j,k} \log \sigma(q_{ijk}\theta_{ijk}^{[m]}) + \frac{1}{8} \sum_{i,j,k} (\theta_{ijk} - z_{ijk}^{[m]})^2,$$

where $z_{ijk}^{[m]} = \theta_{ijk}^{[m]} + 4(x_{ijk} - \sigma(\theta_{ijk}^{[m]}))$ or in the form of tensor

$$\mathcal{Z}^{[m]} = \Theta^{[m]} + 4(\mathcal{X} - \sigma(\Theta^{[m]})). \quad (3)$$

In other words, up to a constant depending on $\Theta^{[m]}$, the function $\frac{1}{8}\|\mathcal{Z}^{[m]} - \Theta\|_F^2$ majorizes $-\ell(\mathcal{X}; \Theta)$ at $\Theta^{[m]}$, and this turns our problem into a simple CP decomposition problem with $\mathcal{Z}^{[m]}$ in the next iteration:

$$\begin{aligned} \min_{\mu, \mathbf{d}, U, V, W} \quad & \frac{1}{8} \|\mathcal{Z}^{[m]} - \Theta\|_F^2 \\ \text{s.t.} \quad & \Theta = \mu \mathbf{1}_{p_1 p_2 p_3} + \sum_{r \in [R]} d_r \cdot \mathbf{u}_r \circ \mathbf{v}_r \circ \mathbf{w}_r, \\ & \mathbf{u}_r^T \mathbf{u}_r = 1, \mathbf{v}_r^T \mathbf{v}_r = 1, \mathbf{w}_r^T \mathbf{w}_r = 1, \text{ and } d_r > 0 \text{ for } r \in [R]. \end{aligned} \quad (4)$$

As the number of iterations grows, $-\ell(\mathcal{X}; \Theta^{[m]})$ decreases and it converges to a local minimum of $-\ell(\mathcal{X}; \Theta)$, the loss function for logistic tensor decomposition as $m \rightarrow \infty$.

There exist various approaches for a CP decomposition of real-valued tensors. Among those, we will consider the Alternating Least Squares (ALS) method (Harshman, 1970; Carroll and Chang, 1970) and the Tensor Power (TP) method (Allen, 2012) to solve the CP decomposition problem (4) in each iteration.

3.2.1 Alternating Least Squares Method

The ALS approach optimizes one factor matrix while treating all the other factor matrices as constants and alternates this optimization procedure over each of the factor matrices repeatedly until some convergence criterion is satisfied.

To solve the CP decomposition problem (4) at the m th step, we update parameters $(\mu, \mathbf{d}, U, V, W)$ in a block coordinate-wise manner. Given (\mathbf{d}, U, V, W) at step m , we compute $\Theta_c^{[m]} = \sum_{r \in [R]} \hat{d}_r^{[m]} \cdot \hat{\mathbf{u}}_r^{[m]} \circ \hat{\mathbf{v}}_r^{[m]} \circ \hat{\mathbf{w}}_r^{[m]}$ first and update μ by taking the average of $\mathcal{Z}^{[m]} - \Theta_c^{[m]}$. With this updated $\hat{\mu}^{[m+1]}$, we define

$$\mathcal{Z}_c^{[m]} = \mathcal{Z}^{[m]} - \hat{\mu}^{[m+1]} \mathbf{1}_{p_1 p_2 p_3} \quad (5)$$

as offset adjusted working variables. To update \mathbf{d}, U, V , and W , we minimize

$$\|\mathcal{Z}_c^{[m]} - \sum_{r \in [R]} d_r \cdot \mathbf{u}_r \circ \mathbf{v}_r \circ \mathbf{w}_r\|_F^2. \quad (6)$$

Given factor matrices V and W , we define $A := U \text{diag}(\mathbf{d})$, and rewrite the above problem in matrix form as a linear least squares problem for A as follows:

$$\min_A \|\mathcal{Z}_{c(1)}^{[m]} - A(W \odot V)^T\|_F^2.$$

Then it can be shown that

$$\hat{A} = \mathcal{Z}_{c(1)}^{[m]}[(W \odot V)^T]^\dagger,$$

where $[(W \odot V)^T]^\dagger$ indicates the Moore-Penrose pseudo-inverse of $(W \odot V)^T \in \mathbb{R}^{R \times p_2 p_3}$ (Golub and van Loan, 1996). To avoid the pseudo-inverse of a large matrix, we can rewrite the above solution as

$$\hat{A} = \mathcal{Z}_{c(1)}^{[m]}[(W \odot V)^T]^\dagger = \mathcal{Z}_{c(1)}^{[m]}(W \odot V)(W^T W * V^T V)^\dagger,$$

where $W^T W * V^T V \in \mathbb{R}^{R \times R}$ is typically smaller. To obtain \hat{U} and $\hat{\mathbf{d}}$, we let $\hat{d}_r = \|\hat{\mathbf{a}}_r\|_2$ and $\hat{\mathbf{u}}_r = \hat{\mathbf{a}}_r / \|\hat{\mathbf{a}}_r\|_2$ for $r \in [R]$. Similarly, we could define $B := V \text{diag}(\mathbf{d})$ and $C := W \text{diag}(\mathbf{d})$ and obtain

$$\hat{B} = \mathcal{Z}_{c(2)}^{[m]}[(U \odot W)^T]^\dagger = \mathcal{Z}_{c(2)}^{[m]}(U \odot W)(U^T U * W^T W)^\dagger$$

and

$$\hat{C} = \mathcal{Z}_{c(3)}^{[m]}[(U \odot V)^T]^\dagger = \mathcal{Z}_{c(3)}^{[m]}(U \odot V)(U^T U * V^T V)^\dagger$$

given other factor matrices. We normalize each column of \hat{A} , \hat{B} , and \hat{C} to unit length and update \hat{U} , \hat{V} , and \hat{W} alternately. Here we use $\text{Normalize}(U)$ to denote the matrix with normalized columns of matrix U .

This MM approach with the ALS method (MM-ALS) is summarized in Algorithm 2 of Appendix A. While this approach is easy to implement, it may take many iterations to converge, and there is no guarantee for convergence to a global minimum or even a stationary point of problem (4) according to Kolda and Bader (2009). Moreover, inversions of $R \times R$ matrices appear many times in Algorithm 2, so the ALS method will be computational expensive for large rank R . The results of MM-ALS method may contain local optima. We make comparisons with other methods in a simulation study later.

3.2.2 Tensor Power Method with Clustering

As a related approach to ALS, we consider iterative rank-one approximations of $\mathcal{Z}_c^{[m]}$ known as the tensor power method (Allen, 2012) to solve the rank- R tensor decomposition problem (6). It is related to the power method for eigendecomposition (Golub and van Loan, 1996). For a rank-one problem, the logit parameter tensor has representation of

$$\Theta = \mu \mathbf{1}_{p_1 p_2 p_3} + d \cdot \mathbf{u} \circ \mathbf{v} \circ \mathbf{w}. \quad (7)$$

Focusing on rank-one vectors, we aim to solve the following approximation problem:

$$\begin{aligned} \min_{d, \mathbf{u}, \mathbf{v}, \mathbf{w}} \quad & \|\mathcal{Z}_c^{[m]} - d \cdot \mathbf{u} \circ \mathbf{v} \circ \mathbf{w}\|_F^2 \\ \text{s.t.} \quad & \mathbf{u}^T \mathbf{u} = 1, \mathbf{v}^T \mathbf{v} = 1, \mathbf{w}^T \mathbf{w} = 1, \text{ and } d > 0. \end{aligned} \quad (8)$$

Given $\mathbf{u} \in \mathbb{R}^{p_1}$, $\mathbf{v} \in \mathbb{R}^{p_2}$ and $\mathbf{w} \in \mathbb{R}^{p_3}$, the minimizer $d \in \mathbb{R}$ is analytically identified as $d = \mathcal{Z}_c^{[m]} \times_1 \mathbf{u}^T \times_2 \mathbf{v}^T \times_3 \mathbf{w}^T$, and this allows us to rewrite the squared error objective function as

$$\|\mathcal{Z}_c^{[m]} - d \cdot \mathbf{u} \circ \mathbf{v} \circ \mathbf{w}\|_F^2 = \|\mathcal{Z}_c^{[m]}\|_F^2 - \|\mathcal{Z}_c^{[m]} \times_1 \mathbf{u}^T \times_2 \mathbf{v}^T \times_3 \mathbf{w}^T\|_F^2.$$

Then we can recast the above problem (8) as

$$\begin{aligned} \max_{\mathbf{u}, \mathbf{v}, \mathbf{w}} \quad & \mathcal{Z}_c^{[m]} \times_1 \mathbf{u}^T \times_2 \mathbf{v}^T \times_3 \mathbf{w}^T \\ \text{s.t.} \quad & \mathbf{u}^T \mathbf{u} = 1, \mathbf{v}^T \mathbf{v} = 1, \mathbf{w}^T \mathbf{w} = 1. \end{aligned}$$

See Kolda and Bader (2009) for reference. Given \mathbf{v} and \mathbf{w} , (8) can be rewritten as the following subproblem for \mathbf{u} :

$$\begin{aligned} \max_{\mathbf{u}} \quad & \mathbf{u}^T (\mathcal{Z}_c^{[m]} \times_2 \mathbf{v}^T \times_3 \mathbf{w}^T) \\ \text{s.t.} \quad & \mathbf{u}^T \mathbf{u} = 1. \end{aligned}$$

Allen (2012) showed that the above problem has explicit solution of

$$\hat{\mathbf{u}} = \text{Normalize}(\mathcal{Z}_c^{[m]} \times_2 \mathbf{v}^T \times_3 \mathbf{w}^T), \quad (9)$$

which satisfies the Karush–Kuhn–Tucker (KKT) conditions (Boyd and Vandenberghe, 2004).

Again alternating among the three factors, we can update one factor at a time given the other factors to maximize the objective function. For instance, we first update \mathbf{u} given \mathbf{v} and \mathbf{w} , and then update \mathbf{v} and \mathbf{w} respectively in a similar way. Each subproblem in matrixized form can be solved explicitly, and the solutions are given by

$$\begin{aligned} \hat{\mathbf{u}} &= \text{Normalize}(\mathcal{Z}_c^{[m]} \times_2 \mathbf{v}^T \times_3 \mathbf{w}^T), \\ \hat{\mathbf{v}} &= \text{Normalize}(\mathcal{Z}_c^{[m]} \times_1 \mathbf{u}^T \times_3 \mathbf{w}^T), \\ \hat{\mathbf{w}} &= \text{Normalize}(\mathcal{Z}_c^{[m]} \times_1 \mathbf{u}^T \times_2 \mathbf{v}^T). \end{aligned}$$

Then d is updated with $\hat{d} = \mathcal{Z}_c^{[m]} \times_1 \hat{\mathbf{u}}^T \times_2 \hat{\mathbf{v}}^T \times_3 \hat{\mathbf{w}}^T$. Finally, the logit parameter tensor is updated with $\Theta^{[m+1]} = \hat{\mu}^{[m+1]} \mathbf{1}_{p_1 p_2 p_3} + \hat{d} \cdot \hat{\mathbf{u}} \circ \hat{\mathbf{v}} \circ \hat{\mathbf{w}}$, which then gives $\mathcal{Z}^{[m+1]}$ in (3).

For rank R component tensors, we repeat this rank-one decomposition multiple times with different initializations and produce R rank-one component tensors to combine. By repeating the tensor power method with differential initializations for L times, we can obtain L tuples stored in $S = \{(\hat{d}_\tau, \hat{\mathbf{u}}_\tau, \hat{\mathbf{v}}_\tau, \hat{\mathbf{w}}_\tau), \tau \in [L]\}$. Focusing on large estimates of \hat{d}_τ and removing too similar tuples, we further cluster those L tuples into R clusters to produce R distinct rank-one component tensors. Then we reorder the R components with decreasing magnitude of \hat{d}_j , which are the final output of our algorithm. We summarize this MM approximation with Tensor Power method (MM-TP) in Algorithm 1.

The Tensor Power method (TP) can be viewed as a rank-one version of ALS. It only updates one column of each factor matrix in each iteration and does not require matrix inversion, which greatly reduces computational complexity compared to ALS (Anandkumar et al., 2014). Also, as a greedy method, the first few estimated factors by the tensor power method typically explain more deviance than ALS method (Allen, 2012).

Initialization is important for non-convex problems. In order to avoid local optima, Algorithm 1 contains a loop running for L different initializations. Because good initial values are not known in advance, we need to identify them. As suggested in Anandkumar et al. (2014), we

develop an algorithm which clusters L tuples in $S = \{(\hat{d}_\tau, \hat{\mathbf{u}}_\tau, \hat{\mathbf{v}}_\tau, \hat{\mathbf{w}}_\tau), \tau \in [L]\}$ into R clusters $\{(\hat{d}_j, \hat{\mathbf{u}}_j, \hat{\mathbf{v}}_j, \hat{\mathbf{w}}_j), j \in [R]\}$ to obtain the final estimates. This clustering algorithm is described in Algorithm 5. Defining $\hat{\Theta}_c = \sum_{j \in [R]} \hat{d}_j \cdot \hat{\mathbf{u}}_j \circ \hat{\mathbf{v}}_j \circ \hat{\mathbf{w}}_j$ and fixing this portion of Θ in (2), we can obtain the final estimate $\hat{\mu}$ as the solution to (2).

Algorithm 1 MM-Tensor Power algorithm for logistic CP decomposition

- 1: **input:** tensor \mathcal{X} , number of initializations L , and rank R .
 - 2: Initialize with $\hat{\mu}_\tau^{[0]}$ and $(\hat{d}_\tau^{[0]}, \hat{\mathbf{u}}_\tau^{[0]}, \hat{\mathbf{v}}_\tau^{[0]}, \hat{\mathbf{w}}_\tau^{[0]})$ where $\tau \in [L]$. Set $m = 0$.
 - 3: **for** $\tau = 1$ **to** L **do**
 - 4: **repeat**
 - 5: Compute $\mathcal{Z}^{[m]}$ in (3).
 - 6: Update $\hat{\mu}^{[m+1]}$.
 - 7: Compute $\mathcal{Z}_c^{[m]} = \mathcal{Z}^{[m]} - \hat{\mu}^{[m+1]} \mathbf{1}_{p_1 p_2 p_3}$.
 - 8: **repeat**
 - 9: $\mathbf{u}_\tau = \text{Normalize}(\mathcal{Z}_c^{[m]} \times_2 (\mathbf{v}_\tau)^T \times_3 (\mathbf{w}_\tau)^T)$
 - 10: $\mathbf{v}_\tau = \text{Normalize}(\mathcal{Z}_c^{[m]} \times_1 (\mathbf{u}_\tau)^T \times_3 (\mathbf{w}_\tau)^T)$
 - 11: $\mathbf{w}_\tau = \text{Normalize}(\mathcal{Z}_c^{[m]} \times_1 (\mathbf{u}_\tau)^T \times_2 (\mathbf{v}_\tau)^T)$
 - 12: **until** converge
 - 13: Update $(\hat{d}_\tau^{[m+1]}, \hat{\mathbf{u}}_\tau^{[m+1]}, \hat{\mathbf{v}}_\tau^{[m+1]}, \hat{\mathbf{w}}_\tau^{[m+1]})$.
 - 14: $m \leftarrow m + 1$
 - 15: **until** converge
 - 16: Return $\hat{\mu}_\tau$ and $(\hat{d}_\tau, \hat{\mathbf{u}}_\tau, \hat{\mathbf{v}}_\tau, \hat{\mathbf{w}}_\tau)$.
 - 17: **end for**
 - 18: Cluster $\{(\hat{d}_\tau, \hat{\mathbf{u}}_\tau, \hat{\mathbf{v}}_\tau, \hat{\mathbf{w}}_\tau), \tau \in [L]\}$ into R clusters $\{(\hat{d}_j, \hat{\mathbf{u}}_j, \hat{\mathbf{v}}_j, \hat{\mathbf{w}}_j), j \in [R]\}$ by Algorithm 5.
 - 19: **output:** $\hat{\mu}$ and R clusters $\{(\hat{d}_j, \hat{\mathbf{u}}_j, \hat{\mathbf{v}}_j, \hat{\mathbf{w}}_j), j \in [R]\}$.
-

4 Sparse CP Decomposition for Binary Data

4.1 Sparse Logistic CP Decomposition

Based on the formulation of logistic tensor decomposition, we consider two approaches which can produce sparse factor matrices with many zero entries. Similar to sparse logistic PCA and sparse tensor decomposition, when appropriate, sparse factor matrices can describe the latent structure more concisely, and nonzero entries can indicate important variables in each mode. To obtain sparse factor matrices for logistic tensor decomposition, we could add a penalty or constraint on the factor matrices. For example, the ℓ_1 -norm penalty and ℓ_0 -norm penalty have been successfully applied in the problems of penalized matrix decomposition (Witten et al., 2009; Yuan and Zhang, 2013) and penalized tensor decomposition (Allen, 2012; Sun et al., 2017).

Based on the logistic CP decomposition (2), we propose the following *sparse logistic CP decomposition* (SLCPD):

$$\begin{aligned}
\min_{\mu, \mathbf{d}, \mathbf{U}, \mathbf{V}, \mathbf{W}} \quad & -\langle \mathcal{X}, \Theta \rangle + \langle \mathbf{1}_{p_1 p_2 p_3}, \log(\mathbf{1}_{p_1 p_2 p_3} + \exp(\Theta)) \rangle \\
\text{s.t.} \quad & \Theta = \mu \mathbf{1}_{p_1 p_2 p_3} + \sum_{r \in [R]} d_r \cdot \mathbf{u}_r \circ \mathbf{v}_r \circ \mathbf{w}_r, \\
& \mathbf{u}_r^T \mathbf{u}_r = 1, \mathbf{v}_r^T \mathbf{v}_r = 1, \mathbf{w}_r^T \mathbf{w}_r = 1, d_r > 0, \\
& p_1(\mathbf{u}_r) \leq t_{1r}, p_2(\mathbf{v}_r) \leq t_{2r}, p_3(\mathbf{w}_r) \leq t_{3r}, r \in [R],
\end{aligned} \tag{10}$$

where $p_i(\cdot)$ for $i = 1, 2, 3$ are penalty functions for factors, and t_{ir} are tuning parameters. We consider two types of sparsity inducing penalty for each factor: the ℓ_1 -norm and ℓ_0 -norm penalty functions for $p_i(\cdot)$. For the ℓ_1 -norm constrained formulation, $p_1(\mathbf{u}_r) = \|\mathbf{u}_r\|_1$, $p_2(\mathbf{v}_r) = \|\mathbf{v}_r\|_1$ and $p_3(\mathbf{w}_r) = \|\mathbf{w}_r\|_1$. For the ℓ_0 -norm constrained formulation, $p_1(\mathbf{u}_r) = \|\mathbf{u}_r\|_0$, $p_2(\mathbf{v}_r) = \|\mathbf{v}_r\|_0$ and $p_3(\mathbf{w}_r) = \|\mathbf{w}_r\|_0$. This formulation naturally extends sparse logistic PCA (Lee et al., 2010b) and binary matrix biclustering (Lee and Huang, 2014) to higher-order binary tensors.

To solve problem (10), we could update U, V and W in an alternative manner similar to ALS. When V and W are fixed, we could solve a regularized non-convex problem for U . And we could solve for V and W in an analogous manner. However, this regularized alternating least squares approach cannot guarantee that the solution is the global minimizer of the problem (Allen, 2012). Instead, we consider a tensor power method and update each factor in an iterative block-wise manner.

4.2 Majorization-Minimization Approach with ℓ_1 -norm Constraint

In order to simplify problem (10) with the ℓ_1 -norm constraints and obtain a simple analytic solution, we relax the original non-convex equality constraints (e.g., $\mathbf{u}^T \mathbf{u} = 1$), and consider the tensor decomposition problem with convex inequality constraints (e.g., $\mathbf{u}^T \mathbf{u} \leq 1$) (Allen, 2012). Although the objective function is not convex in factor matrices jointly, it is convex in each factor matrix individually with all other factor matrices fixed.

Similar to logistic CP decomposition, we consider a rank-one problem to avoid local minima and the MM algorithm. For a rank-one problem, in the m th step of MM algorithm with $\mathcal{Z}_c^{[m]}$ defined in (5), we have the following relaxation:

$$\begin{aligned} \min_{d, \mathbf{u}, \mathbf{v}, \mathbf{w}} \quad & \|\mathcal{Z}_c^{[m]} - d \cdot \mathbf{u} \circ \mathbf{v} \circ \mathbf{w}\|_F^2 \\ \text{s.t.} \quad & \mathbf{u}^T \mathbf{u} \leq 1, \mathbf{v}^T \mathbf{v} \leq 1, \mathbf{w}^T \mathbf{w} \leq 1, d > 0, \\ & \|\mathbf{u}\|_1 \leq c_1, \|\mathbf{v}\|_1 \leq c_2, \|\mathbf{w}\|_1 \leq c_3, \end{aligned} \tag{11}$$

where $c_i \geq 0$ for $i \in [3]$ are tuning parameters.

The constrained formulation (11) produces a feasible solution if $1 \leq c_i \leq \sqrt{p_i}$ and reduces to the un-regularized version when $c_i = \sqrt{p_i}$. If c_i are chosen appropriately, the solution to the relaxed problem still solves the original problem with the ℓ_2 -norm constraints. See Witten et al. (2009) for detailed arguments. Given \mathbf{v} and \mathbf{w} , the relaxed formulation in (11) can be rewritten as a subproblem for \mathbf{u} :

$$\begin{aligned} \max_{\mathbf{u}} \quad & \mathbf{u}^T (\mathcal{Z}_c^{[m]} \times_2 \mathbf{v}^T \times_3 \mathbf{w}^T) \\ \text{s.t.} \quad & \mathbf{u}^T \mathbf{u} \leq 1, \|\mathbf{u}\|_1 \leq c_1. \end{aligned}$$

This subproblem has explicit solution of

$$\hat{\mathbf{u}} = \text{Normalize}(S(\mathcal{Z}_c^{[m]} \times_2 \mathbf{v}^T \times_3 \mathbf{w}^T, \lambda_1)). \tag{12}$$

Here $S(\cdot, \lambda) = \text{sign}(\cdot)(|\cdot| - \lambda)_+$ is the soft-thresholding operator, and λ_1 is the smallest positive value such that $\|\mathbf{u}\|_1 \leq c_1$. The value of λ_1 can be chosen by a binary search (Witten et al., 2009). We can update \mathbf{v} and \mathbf{w} in a similar manner. This MM approximation with Tensor Soft-thresholding Power method (MM-TSP) is summarized in Algorithm 3 of Appendix A.

4.3 Majorization-Minimization Approach with ℓ_0 -norm Constraint

We propose to solve problem (10) with the ℓ_0 -norm constraints in a manner similar to the tensor power method, and consider iterative rank-one sparse approximations of $\mathcal{Z}_c^{[m]}$ in (5). For a rank-one problem, in the m th step of MM algorithm, we have the following problem:

$$\begin{aligned} \min_{d, \mathbf{u}, \mathbf{v}, \mathbf{w}} \quad & \|\mathcal{Z}_c^{[m]} - d \cdot \mathbf{u} \circ \mathbf{v} \circ \mathbf{w}\|_F^2 \\ \text{s.t.} \quad & \mathbf{u}^T \mathbf{u} = 1, \mathbf{v}^T \mathbf{v} = 1, \mathbf{w}^T \mathbf{w} = 1, d > 0, \\ & \|\mathbf{u}\|_0 \leq s_1, \|\mathbf{v}\|_0 \leq s_2, \|\mathbf{w}\|_0 \leq s_3, \end{aligned} \quad (13)$$

where $s_i \leq p_i$ for $i \in [3]$ are tuning parameters.

The constrained formulation (13) produces a feasible solution if $1 \leq s_i \leq p_i$. It reduces to the un-regularized problem without any constraint in each factor when $s_i = p_i$. Inspired by Yuan and Zhang (2013); Sun et al. (2017), we could apply the tensor truncated power method in solving the above problem. Given \mathbf{v} and \mathbf{w} , the constrained problem can be rewritten as a subproblem for \mathbf{u} :

$$\begin{aligned} \max_{\mathbf{u}} \quad & \mathbf{u}^T (\mathcal{Z}_c^{[m]} \times_2 \mathbf{v}^T \times_3 \mathbf{w}^T) \\ \text{s.t.} \quad & \mathbf{u}^T \mathbf{u} = 1, \|\mathbf{u}\|_0 \leq s_1, \end{aligned}$$

where s_1 denotes the number of non-zero entries. This subproblem has explicit solution of

$$\hat{\mathbf{u}} = \text{Normalize}(T(\mathcal{Z}_c^{[m]} \times_2 \mathbf{v}^T \times_3 \mathbf{w}^T, s_1)). \quad (14)$$

Here $T(\cdot, s)$ is the truncation operator which keeps the largest $\lfloor s \rfloor$ entries of a vector in the absolute value and truncates the remaining entries to zero. We can update \mathbf{v} and \mathbf{w} in a similar manner. This MM approximation with Tensor Truncated Power method (MM-TTP) is summarized in Algorithm 4 of Appendix.

5 Missing Data and Tensor Completion

In practice, missing data is common. To handle missing data, we extend our algorithms. Given data tensor \mathcal{X} of size $p_1 \times p_2 \times p_3$, we let $\Omega = \{(i, j, k) \in [p_1] \times [p_2] \times [p_3] | x_{ijk} \text{ is observed}\}$ denote the index set of observed entries. Given $\Omega \subseteq [p_1] \times [p_2] \times [p_3]$, we can define the projection operation $\mathcal{P}_\Omega : \mathbb{R}^{p_1 \times p_2 \times p_3} \mapsto \mathbb{R}^{p_1 \times p_2 \times p_3}$ as follows:

$$\mathcal{P}_\Omega(\mathcal{X}) = \begin{cases} x_{ijk} & \text{if } (i, j, k) \in \Omega \\ 0 & \text{if } (i, j, k) \notin \Omega. \end{cases}$$

\mathcal{P}_Ω replaces the missing entries in the data tensor \mathcal{X} with zeros, and leaves the observed entries unchanged. Let $\mathcal{H} = (h_{ijk}) \in \mathbb{R}^{p_1 \times p_2 \times p_3}$ be a masking tensor such that $\mathcal{P}_\Omega(\mathcal{X}) = \mathcal{H} * \mathcal{X}$, where $*$ denotes the Hadamard product of two tensors. Then for partially observed data, we can redefine the following rank- R logistic CP decomposition problem:

$$\begin{aligned} \min_{\mu, d, U, V, W} \quad & -\langle \mathcal{H} * \mathcal{X}, \Theta \rangle + \langle \mathcal{H}, \log(\mathbf{1}_{p_1 p_2 p_3} + \exp(\Theta)) \rangle \\ \text{s.t.} \quad & \Theta = \mu \mathbf{1}_{p_1 p_2 p_3} + \sum_{r \in [R]} d_r \cdot \mathbf{u}_r \circ \mathbf{v}_r \circ \mathbf{w}_r, \\ & \mathbf{u}_r^T \mathbf{u}_r = 1, \mathbf{v}_r^T \mathbf{v}_r = 1, \mathbf{w}_r^T \mathbf{w}_r = 1, \text{ and } d_r > 0 \text{ for } r \in [R]. \end{aligned} \quad (15)$$

To solve the above problem, we modify the previous algorithms by introducing new working variables. We define new working variables $\mathcal{Y}^{[m]} = (y_{ijk}^{[m]})$ by filling in the missing values with fitted values based on the current estimate of logit parameter tensor Θ as follows:

$$y_{ijk}^{[m]} = \begin{cases} z_{ijk}^{[m]} & (i, j, k) \in \Omega \\ \theta_{ijk}^{[m]} & (i, j, k) \notin \Omega, \end{cases} \quad (16)$$

where $\mathcal{Z}^{[m]} = \Theta^{[m]} + 4(\mathcal{X} - \sigma(\Theta^{[m]}))$. In the m th step of MM approximation, the objective function of problem (2) turns into $\frac{1}{8}\|\mathcal{Y}^{[m]} - \Theta\|_F^2$. For sparse logistic CP decomposition, we could also replace the working variables $\mathcal{Z}^{[m]}$ with $\mathcal{Y}^{[m]}$ in the MM approximation of regularized problem (10).

Once we have $\hat{\Theta}$ from observed data, we can use it for missing value prediction. After estimating $\hat{\Theta}$ from observed data as in (15), we could predict the missing entries of \mathcal{X} by using $\hat{\mathcal{P}} = \text{logit}^{-1}(\hat{\Theta})$, where $\hat{\mathcal{P}} = (\hat{p}_{ijk})$ is the tensor with estimated probabilities of Bernoulli random variables. For probability $\hat{p}_{ijk} \geq 0.5$, we could impute missing x_{ijk} with one and zero otherwise. Similar ideas of such tensor completion for continuous data and binary data have been investigated in Acar et al. (2011) and Wang and Li (2020).

6 Selecting Rank and Tuning Parameters

Selecting an appropriate rank for tensor decomposition is an issue of practical importance. However, there has been few discussions in the literature. Allen (2012); Sun et al. (2017); Wang and Li (2020) derived a BIC heuristic to select the rank and degree of sparsity for CP decomposition. The consistency of BIC in binary tensor decomposition is unknown, but similar problems have been investigated by Shi et al. (2019) in the context of relational learning. Alternatively, we could use cross-validation to choose the rank and tuning parameters, but cross-validation can be slow to carry out for high-dimensional tensors. Shen and Huang (2008); Witten et al. (2009); Udell et al. (2016) have used cross-validation to select the rank and sparsity tuning parameters for matrix decomposition problems. In this section, we investigate AIC, BIC, cross-validation and explained deviance as possible approaches to select the rank and tuning parameters. These approaches are illustrated with simulated data in Appendix B.

6.1 BIC and AIC

As the tuning parameters c_i or s_i decrease, the estimated factor matrices become sparser, and the model for the underlying logit parameter tensor becomes simpler and easier to interpret. To reach a balance between model complexity and goodness of fit, we adopt the Bayesian information criterion (BIC) to select the optimal penalty parameter in sparse logistic tensor decomposition.

Given a prespecified set of rank values and penalty parameter values c_i or cardinality values s_i , we choose the combination of parameters $(\hat{R}, \hat{c}_1, \hat{c}_2, \hat{c}_3)$ or $(\hat{R}, \hat{s}_1, \hat{s}_2, \hat{s}_3)$ which minimizes the BIC criterion for sparse logistic CP decomposition $\hat{\Theta}$ in (10):

$$\text{BIC} := -2\ell(\mathcal{X}; \hat{\Theta}) + \log(p_1 p_2 p_3) \times (1 + \|\hat{U}\|_0 + \|\hat{V}\|_0 + \|\hat{W}\|_0 - 2R). \quad (17)$$

Here $\|\hat{U}\|_0$ is the number of nonzero entries in matrix \hat{U} when the penalty parameter is \hat{c}_1 or cardinality parameter is \hat{s}_1 , and $\|\hat{V}\|_0$ and $\|\hat{W}\|_0$ are defined analogously. Note that $\hat{\mu}$ has $df = 1$, $\hat{\mathbf{d}}$ has $df = R$ and there are $3R$ constraints on $(\hat{U}, \hat{V}, \hat{W})$, so the overall df of the logit tensor model can be taken as $1 + \|\hat{U}\|_0 + \|\hat{V}\|_0 + \|\hat{W}\|_0 - 2R$. This is analogous to the way the model degrees of freedom is defined for sparse logistic PCA.

For the case with missing data, letting Ω denote the index set of observed entries, we use $|\Omega|$ rather than $p_1p_2p_3$, and the log likelihood for the observed entries in Ω is defined as $\ell(\mathcal{X}_\Omega; \Theta) := \sum_{ijk \in \Omega} \ell(x_{ijk}; \theta_{ijk})$ in the BIC. This leads to the following extended BIC:

$$\text{BIC}_\Omega := -2\ell(\mathcal{X}_\Omega; \hat{\Theta}) + \log(|\Omega|) \times (1 + \|\hat{U}\|_0 + \|\hat{V}\|_0 + \|\hat{W}\|_0 - 2R).$$

Note that for fully observed data, $|\Omega| = p_1p_2p_3$ and $\ell(\mathcal{X}_\Omega; \Theta) = \ell(\mathcal{X}; \Theta)$, and the extended BIC reduces to (17).

To select the optimal tuning parameters, we could also consider minimizing the Akaike information criterion (AIC) for tensor decomposition:

$$\text{AIC} := -2\ell(\mathcal{X}; \hat{\Theta}) + 2 \times (1 + \|\hat{U}\|_0 + \|\hat{V}\|_0 + \|\hat{W}\|_0 - 2R). \quad (18)$$

Given a fixed rank R , we first search for the optimal tuning parameters $(\hat{c}_1, \hat{c}_2, \hat{c}_3)$ or $(\hat{s}_1, \hat{s}_2, \hat{s}_3)$ by BIC/AIC, and then given the tuning parameter values, we seek the best rank R which minimizes BIC/AIC.

6.2 Cross-validation

Cross-validation has been proven to be useful in selecting tuning parameters in many settings. We could also select the rank and sparsity penalty parameters by an approach similar to cross-validation since our algorithms can handle missing data. However, compared with BIC or AIC, cross-validation is computationally more expensive. Many metrics could be used for cross-validation in binary tensor decomposition. We cross-validate each tuning parameter value by minimizing the negative log likelihood, $-\ell(\mathcal{X}; \Theta)$ in this paper.

For a 5-fold cross-validation of rank R , we randomly split binary tensor entries into 5 folds: 4 folds are used for training and 1 fold is used for testing, where nonzero entries and zero entries are split separately with the same ratio. For a fixed rank R , we treat the test data as missing data and estimate Θ by minimizing the negative log likelihood $-\ell(\mathcal{X}_{\text{train}}; \Theta)$ with the training data $\mathcal{X}_{\text{train}}$ only. Then for evaluation of $\hat{\Theta}$, we calculate the negative log likelihood $-\ell(\mathcal{X}_{\text{test}}; \hat{\Theta})$ using the test data $\mathcal{X}_{\text{test}}$. We repeat the above process for five times and obtain the average negative log likelihood for each rank. A similar process can be used to select the levels of sparsity in factor matrices.

6.3 Explained Deviance

Alternatively, we could also use the explained deviance for determining the rank and tuning parameter values analogous to the use of explained total variance in standard PCA. The deviance of estimated logit parameter tensor $\hat{\Theta}$ based on data \mathcal{X} is defined as $D(\mathcal{X}; \hat{\Theta}) = -2(\ell(\mathcal{X}; \hat{\Theta}) - \ell(\mathcal{X}; \Theta_S))$, where Θ_S is the logit parameter tensor of the saturated model. For binary tensor \mathcal{X} , $\Theta_S = \text{logit}(\mathcal{X})$, where $\text{logit}(x) = \log(\frac{x}{1-x})$ is taken elementwise, and thus $\ell(\mathcal{X}; \Theta_S) = 0$. This leads to $D(\mathcal{X}; \hat{\Theta}) = -2\ell(\mathcal{X}; \hat{\Theta})$, and we have

$$D(\mathcal{X}; \hat{\Theta}) := -2\langle \mathcal{X}, \hat{\Theta} \rangle + 2\langle \mathbf{1}_{p_1p_2p_3}, \log(\mathbf{1}_{p_1p_2p_3} + \exp(\hat{\Theta})) \rangle.$$

For partially observed data \mathcal{X}_Ω , the deviance can be expressed as

$$D(\mathcal{X}_\Omega; \hat{\Theta}) := -2\langle \mathcal{H} * \mathcal{X}, \hat{\Theta} \rangle + 2\langle \mathcal{H}, \log(\mathbf{1}_{p_1p_2p_3} + \exp(\hat{\Theta})) \rangle$$

using the masking tensor \mathcal{H} defined previously.

Let $\widehat{\Theta}_0 := \widehat{\mu} \mathbf{1}_{p_1 p_2 p_3}$ as an estimated tensor with offset term μ only, and for $r \in [R]$, let $\widehat{\Theta}_r := \widehat{\mu} \mathbf{1}_{p_1 p_2 p_3} + \sum_{i=1}^r \widehat{d}_i \cdot \widehat{\mathbf{u}}_i \circ \widehat{\mathbf{v}}_i \circ \widehat{\mathbf{w}}_i$ with the first r components. We call $D(\mathcal{X}_\Omega; \widehat{\Theta}_0)$ the null deviance and define the cumulative percentage of explained deviance of the first r components as

$$1 - \frac{D(\mathcal{X}_\Omega; \widehat{\Theta}_r)}{D(\mathcal{X}_\Omega; \widehat{\Theta}_0)}.$$

Similarly, we define the marginal percentage of explained deviance by the r th component as

$$\frac{D(\mathcal{X}_\Omega; \widehat{\Theta}_{r-1}) - D(\mathcal{X}_\Omega; \widehat{\Theta}_r)}{D(\mathcal{X}_\Omega; \widehat{\Theta}_0)}.$$

These criteria extend the proportion of total variance explained in real-valued tensors (Allen, 2012) to binary tensors. The same criteria have been considered in the context of binary matrix factorization (Landgraf and Lee, 2020a).

We could also define the marginal deviance of the r th component as

$$D_r := D(\mathcal{X}; \widehat{\Theta}_{(r)}) = -2\langle \mathcal{X}, \widehat{\Theta}_{(r)} \rangle + 2\langle \mathbf{1}_{p_1 p_2 p_3}, \log(\mathbf{1}_{p_1 p_2 p_3} + \exp(\widehat{\Theta}_{(r)})) \rangle,$$

where $\widehat{\Theta}_{(r)} := \widehat{\mu} \mathbf{1}_{p_1 p_2 p_3} + \widehat{d}_r \cdot \widehat{\mathbf{u}}_r \circ \widehat{\mathbf{v}}_r \circ \widehat{\mathbf{w}}_r$. As index r corresponds to weight d_r ordered from largest to smallest, typically the r th marginal deviance will increase as r increases. Therefore the first component with largest weight d_1 will have the smallest marginal deviance D_1 , and the last component with smallest weight d_R will have the largest marginal deviance D_R .

7 Simulation Study

We compare the proposed ℓ_0 -norm constrained logistic tensor decomposition with Tensor Truncated Power (TTP) method, ℓ_1 -norm constrained logistic tensor decomposition with Tensor Soft-thresholding Power (TSP) method, and un-regularized logistic tensor decomposition with Tensor Power (TP) method and Alternating Least Squares (ALS) method. We have implemented all methods in R (R Core Team, 2019) using the `rTensor` package (Li et al., 2018) for efficient tensor computations. Appendix C describes implementational details including initialization and termination of the proposed algorithms as well as the clustering procedure.

7.1 Simulation Setup

To generate binary tensor data \mathcal{X} with sparse logit parameters, we first specify the underlying logit parameter tensor Θ^* of size $p_1 \times p_2 \times p_3$. We consider the following four scenarios for the size and rank of Θ^* :

- I. $p_1 = 1000, p_2 = 10, p_3 = 10$, and $R = 1$; II. $p_1 = 1000, p_2 = 10, p_3 = 10$, and $R = 2$;
- III. $p_1 = 1000, p_2 = 100, p_3 = 10$, and $R = 1$; IV. $p_1 = 1000, p_2 = 100, p_3 = 10$, and $R = 2$.

In all simulation settings, we keep the level of sparsity equal in each dimension by setting the cardinality of nonzero entries as $p_{0j} = 0.2p_j$ for $j = 1, 2, 3$. With fixed dimensionality (p_1, p_2, p_3) and true rank R , we first generate independent and identically distributed standard Gaussian entries for three factor matrices $U \in \mathbb{R}^{p_1 \times R}$, $V \in \mathbb{R}^{p_2 \times R}$ and $W \in \mathbb{R}^{p_3 \times R}$. Then to induce sparsity in the factor matrices with fixed cardinality parameters (p_{01}, p_{02}, p_{03}) , we truncate some entries in each column of U, V and W to zero. Finally, we normalize each column of U, V and W to get U^*, V^* and W^* .

To specify the weights d_1^*, \dots, d_R^* properly, we first consider their null values when $\Theta = (0)$ or $\mathcal{P} = (1/2)$, taken as the baseline noise level, and then determine their actual values proportionally.

To find such null values, we first generate a $p_1 \times p_2 \times p_3$ binary tensor whose entries are mutually independent realizations from a Bernoulli distribution with $p = 1/2$. We carry out a rank- R logistic CP decomposition (2) of the binary tensor and calculate the average of R weights denoted by d_b . We repeat this process for 100 times and take the mean of d_b as the baseline noise level. Then using d_b , we could define the signal-to-noise ratio (SNR) as $\text{SNR}_r = d_r^*/d_b$ to determine the weights d_r^* for $r \in [R]$.

We consider different combinations of signal-to-noise ratio values: $\text{SNR} = (5, 3)$ when $R = 2$, and $\text{SNR} = 3$ when $R = 1$. With specified weights, we define the logit parameter tensor as

$$\Theta^* = \mu^* \mathbf{1}_{p_1 p_2 p_3} + \sum_{r \in [R]} d_r^* \cdot \mathbf{u}_r^* \circ \mathbf{v}_r^* \circ \mathbf{w}_r^*,$$

which extends the spiked tensor model (Montanari and Richard, 2014) to binary data. The overall logit parameter μ^* is set to zero. Because of the sparsity in $(\mathbf{u}_r^*, \mathbf{v}_r^*, \mathbf{w}_r^*)$ for $r \in [R]$, Θ^* is also sparse. Finally, we generate x_{ijk} from $\text{Bernoulli}(p_{ijk}^*)$, where $p_{ijk}^* = \text{logit}^{-1}(\theta_{ijk}^*)$ for $i \in [p_1]$, $j \in [p_2]$, $k \in [p_3]$, and obtain a binary tensor $\mathcal{X} = (x_{ijk})$ with the corresponding probability tensor $\mathcal{P}^* = (p_{ijk}^*)$.

As for tuning parameters in this simulation study, we parameterize $c_j = \sqrt{p_j} \times c$ ($j = 1, 2, 3$) for the ℓ_1 -norm constraint and $s_j = p_j \times s$ for the ℓ_0 -norm constraint. To make the ℓ_1 -norm and ℓ_0 -norm problems well-defined, we vary the ratio $c \in [\max_i \frac{1}{\sqrt{p_i}}, 1]$ for the ℓ_1 -norm constraint and ratio $s \in [\max_i \frac{1}{p_i}, 1]$ for the ℓ_0 -norm constraint. For the numerical results in Table 1, we considered a prespecified set of rank values $\{1, \dots, 4\}$ and a range of values for the ratio parameters c and s and tuned the parameters using AIC. In simulation settings where true factors $\mathbf{u}^*, \mathbf{v}^*$ and \mathbf{w}^* are known, we could set $(s_1, s_2, s_3) = (\|\mathbf{u}^*\|_0, \|\mathbf{v}^*\|_0, \|\mathbf{w}^*\|_0)$ and $(c_1, c_2, c_3) = (\|\mathbf{u}^*\|_1, \|\mathbf{v}^*\|_1, \|\mathbf{w}^*\|_1)$ as optimal tuning parameters in the ℓ_0 -norm and ℓ_1 -norm problems, respectively.

7.2 True Positive Rate and False Positive Rate

When the true logit parameters are sparse, we are interested in recovering the sparse pattern and selecting important nonzero features in the latent factors. The selection performance can be measured by the true positive rate (TPR): the proportion of correctly estimated non-zeros in the true parameter and the false positive rate (FPR): the proportion of true zeros that are incorrectly estimated to be nonzero. For an estimated factor matrix \hat{U} , the TPR and FPR are defined as

$$\text{TPR}_{\hat{U}} = \frac{1}{r} \sum_{r \in [R]} \frac{|\{i : (\hat{\mathbf{u}}_r)_i \neq 0 \text{ and } (\mathbf{u}_r^*)_i \neq 0\}|}{|\{i : (\mathbf{u}_r^*)_i \neq 0\}|}$$

and

$$\text{FPR}_{\hat{U}} = \frac{1}{r} \sum_{r \in [R]} \frac{|\{i : (\hat{\mathbf{u}}_r)_i \neq 0 \text{ and } (\mathbf{u}_r^*)_i = 0\}|}{|\{i : (\mathbf{u}_r^*)_i = 0\}|},$$

respectively. For \hat{V} and \hat{W} , $\text{TPR}_{\hat{V}}$, $\text{TPR}_{\hat{W}}$, $\text{FPR}_{\hat{V}}$ and $\text{FPR}_{\hat{W}}$ can be defined analogously. Then the overall TPR and FPR for $\hat{\Theta}$ can be defined as $\text{TPR}(\hat{\Theta}) = (\text{TPR}_{\hat{U}} + \text{TPR}_{\hat{V}} + \text{TPR}_{\hat{W}})/3$ and $\text{FPR}(\hat{\Theta}) = (\text{FPR}_{\hat{U}} + \text{FPR}_{\hat{V}} + \text{FPR}_{\hat{W}})/3$.

7.3 Estimation Errors

To evaluate the accuracy of $\hat{\Theta} = \hat{\mu}\mathbf{1}_{p_1 p_2 p_3} + \sum_{r=1}^R \hat{d}_r \cdot \hat{\mathbf{u}}_r \circ \hat{\mathbf{v}}_r \circ \hat{\mathbf{w}}_r$ in recovering the true logit parameter tensor Θ^* , we look at its root mean squared error (RMSE) defined as

$$\text{RMSE}(\hat{\Theta}) = \frac{1}{\sqrt{p_1 p_2 p_3}} \|\hat{\Theta} - \Theta^*\|_F.$$

To measure the quality of the estimated components and weights in tensor decomposition separately, we also calculate the mean vector estimation error and weight estimation error (Anandkumar et al., 2014; Sun et al., 2017):

$$\text{Mean Error} = \frac{1}{3} \{\text{ME}_{\hat{U}} + \text{ME}_{\hat{V}} + \text{ME}_{\hat{W}}\},$$

and

$$\text{Weight Error} = \frac{\|\hat{\mathbf{d}} - \mathbf{d}^*\|_2}{\|\mathbf{d}^*\|_2},$$

where $\text{ME}_{\hat{U}} = \frac{1}{R} \sum_{r \in [R]} \min\{\|\hat{\mathbf{u}}_r - \mathbf{u}_r^*\|_2, \|\hat{\mathbf{u}}_r + \mathbf{u}_r^*\|_2\}$, $\text{ME}_{\hat{V}}$ and $\text{ME}_{\hat{W}}$ are defined analogously. Operating characteristics of these evaluation metrics are illustrated with simulated data in Appendix B.

7.4 Comparisons

We compare the proposed ℓ_0 -norm logistic tensor decomposition with TTP method, ℓ_1 -norm logistic tensor decomposition with TSP method, and un-regularized logistic tensor decomposition method with ALS, TP and block relaxation (BR) (Wang and Li, 2020) methods by calculating the average mean squared error, mean estimation error, weight estimation error and TPR/FPR over 20 random replicates simulated from the four scenarios. Table 1 presents the results with standard error in parentheses.

The columns for TPR and FPR indicate that the use of ℓ_1 -norm and ℓ_0 -norm constraints can lead to correct identification of nonzero entries in the logit tensor with FPR close to 0 and TPR mostly 80% to 90%. Regularized estimates tend to have smaller errors on average in terms of RMSE, mean vector estimation error and weight estimation error. In particular, ℓ_1 -norm regularized estimates with TSP method have minimum errors on the whole. Table 1 suggests that sparse logistic tensor decompositions indeed have better performance than their non-sparse counterpart when the true factor matrices are sparse.

We also compare the five methods computationally in terms of the number of iterations and run time. For comparison, we ran all methods on the same data simulated from scenario 3 with rank-one decomposition using the same initialization and repeated the process 10 times. Table 2 shows the average run time in seconds and number of iterations. Their standard errors are in parentheses. The time for clustering is ignored. Computing was done on a laptop with a 2.7 GHz processor and 8 GB of memory. The times for TSP and TTP methods correspond to the optimal tuning parameters. Note that the run time varies with different initializations, which result in relatively large standard errors. According to Table 2, TP is faster than ALS, and TSP and TTP take more time to converge than the un-regularized TP method. For time per iteration, we find all methods based on tensor power method are faster than ALS. And among all tensor power methods, TTP is the slowest due to truncation. Notably, the block relaxation approach to logistic tensor decomposition using iteratively reweighted least squares method takes significantly longer than the proposed MM approach.

Table 1: Comparisons of five logistic tensor decomposition methods under four simulation settings. The minimum value for each error measure is highlighted in bold, and the numbers in parentheses are standard errors.

Scenario	Method	RMSE(Θ)	Mean Error	Weight Error	TPR	FPR
1	BR	0.3683 (0.0675)	0.8651 (0.3601)	0.5649 (0.1469)	1 (0)	1 (0)
	ALS	0.3255 (0.0159)	0.5418 (0.0465)	0.5600 (0.0272)	1 (0)	1 (0)
	TP	0.3450 (0.0146)	0.6279 (0.0413)	0.5590 (0.0338)	1 (0)	1 (0)
	TSP	0.1744 (0.0312)	0.2832 (0.0265)	0.0347 (0.0255)	0.8916 (0.0083)	0.0208 (0.0041)
	TTP	0.2877 (0.0028)	0.3922 (0.0021)	0.5405 (0.0029)	0.9000 (0.0000)	0.0250 (0.0000)
2	BR	0.6815 (0.0592)	0.6911 (0.1768)	0.6266 (0.1362)	1 (0)	1 (0)
	ALS	0.6504 (0.0309)	0.6932 (0.1740)	0.6283 (0.0170)	1 (0)	1 (0)
	TP	0.7353 (0.0276)	0.5534 (0.0347)	0.6049 (0.0238)	1 (0)	1 (0)
	TSP	0.6491 (0.0627)	0.4150 (0.1095)	0.1994 (0.0068)	0.8791 (0.0291)	0.0208 (0.0020)
	TTP	0.7195 (0.0507)	0.6478 (0.2754)	0.5629 (0.0413)	0.7083 (0.2250)	0.0729 (0.2250)
3	BR	0.1545 (0.0112)	0.5192 (0.0420)	0.2957 (0.0444)	1 (0)	1 (0)
	ALS	0.1842 (0.0102)	0.6017 (0.0286)	0.4970 (0.0209)	1 (0)	1 (0)
	TP	0.1914 (0.0123)	0.6456 (0.0351)	0.4920 (0.0296)	1 (0)	1 (0)
	TSP	0.1451 (0.0180)	0.4197 (0.0495)	0.1225 (0.0981)	0.7900 (0.0200)	0.0137 (0.0070)
	TTP	0.1523 (0.0101)	0.4296 (0.0149)	0.4289 (0.0294)	0.8708 (0.0225)	0.0322 (0.0225)
4	BR	0.3951 (0.0142)	0.4248 (0.0164)	0.3081 (0.0168)	1 (0)	1 (0)
	ALS	0.3930 (0.0179)	0.5733 (0.0162)	0.5841 (0.0113)	1 (0)	1 (0)
	TP	0.4344 (0.0162)	0.5560 (0.0158)	0.4561 (0.0182)	1 (0)	1 (0)
	TSP	0.3911 (0.0152)	0.3590 (0.0120)	0.1985 (0.0218)	0.8591 (0.0066)	0.0053 (0.0038)
	TTP	0.4155 (0.0145)	0.4088 (0.0172)	0.4207 (0.0371)	0.9358 (0.0025)	0.0160 (0.0025)

Table 2: Comparison of the average run time (in seconds) and number of iterations for five logistic tensor decomposition methods under scenario 3.

METHOD	TIME	ITERATION NUMBER	TIME PER ITERATION
BR	59.1640 (0.8690)		
ALS	8.9147 (1.4783)	12.3 (4.2322)	2.7853 (0.7180)
TP	6.3479 (2.1182)	25.1 (6.7797)	0.2336 (0.0221)
TSP	10.8628 (4.4506)	36.0 (11.6961)	0.2545 (0.0490)
TTP	10.9305 (4.3180)	12.6 (0.7023)	0.9083 (0.3570)

8 Analysis of Nations Data

This section investigates the efficacy of our methods on transposable binary tensor data. The nations dataset (Rummel, 1968) we consider includes 14 countries and 54 binary predicates (e.g. *treaties*, *exports*) representing interactions between countries. Kemp et al. (2006) thresholded each continuous variable at its mean and created a binary tensor of size $14 \times 14 \times 56$. This tensor consists of 56 political relations of 14 countries between 1950 and 1965. Each entry in the tensor (*nation*, *nation*, *relation*) indicates the presence or absence of a political relation. If nation i and nation j have relation k , $x_{ijk} = 1$ and otherwise $x_{ijk} = 0$.

The relationship between a nation and itself is not well defined, so we exclude the diagonal elements x_{iik} and treat them as missing entries. Overall the missing rate is 11.1%. This dataset has been investigated by Kemp et al. (2006); Nickel et al. (2011); Wang and Li (2020). Different from the previous analysis, we incorporate an offset term μ for the logit parameter tensor and impose a sparsity penalty on factor matrices.

The goals for this data analysis are grouping nations and relations, and identifying potential blocks of nations and relations. For example, we are interested in finding relations that exist significantly for certain groups of nations, or that can help to distinguish different groups of nations. Appendix D gives provides more results of data analysis.

8.1 Visualization of Factors

Due to the special structure of the nations data, we consider a special logistic CP decomposition with the same first two modes \mathbf{u} and \mathbf{v} . More specifically, we impose the additional constraints $\mathbf{u}_r = \mathbf{v}_r$ for $r \in [R]$ in standard logistic CP decomposition in (2). To maintain this special structure, we keep the original update of \mathbf{u} and \mathbf{w} but set $\mathbf{v} = \mathbf{u}$ for the update of \mathbf{v} in the tensor power method.

To decide a proper rank of logistic CP decomposition, we fit a rank-14 logistic CP decomposition first. We find that there are 3 weights much larger than other weights as shown in Figure 1 and the offset term μ is estimated to be -1.69 . In Figure 1, the scree plot of marginal explained deviance suggests $R = 4$. Based on the information, we conclude that a rank-4 logistic CP decomposition is reasonable for the nations data.

To get a better understanding of factors, we apply K -means clustering (MacQueen, 1967; Lloyd, 1982) on the estimated factors for the nations and relations, and visualize them in Figures 2 and 3. The estimated number of clusters can be determined by BIC criterion, where $K = 3$ is chosen for the nation factors, and $K = 5$ is chosen for the relation factors. The three clusters of nations contain communist countries (*USSR*, *Poland*, *Cuba*, *China*), western countries (*USA*, *UK*, *Netherlands*, *Brazil*), and neutral countries. The relations are grouped into five clusters. Three major clusters regard i) negative/hostile actions (e.g., *warning*, *protests*, *accusation*, *military actions*), ii) international partnerships through intergovernmental organizations and NGOs (e.g., *intergov-orgs*, *relngo*, *ngo*), and iii) exports and population exchanges (e.g., *exportbook*, *exports*, *students*, *emigrants*). The remaining two minor clusters are defined by the nation’s common bloc membership: opposing common bloc membership (*commonbloc0*, *blockpositionindex*, *weightedunvote*) and different common bloc membership (*commonbloc1*).

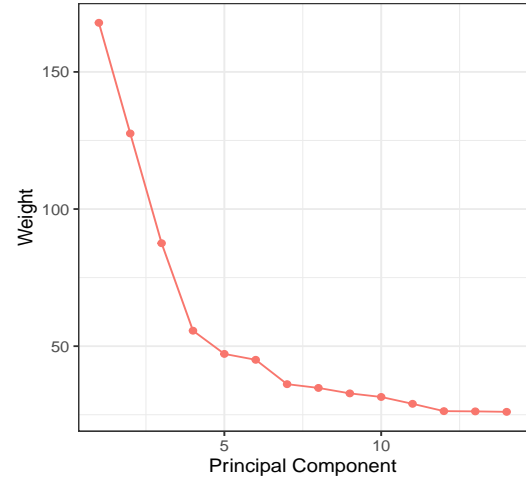
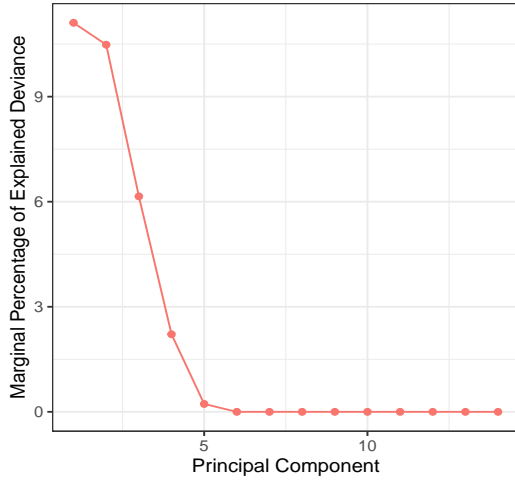


Figure 1: Explained deviance and weight versus the number of principal components for the nations data.

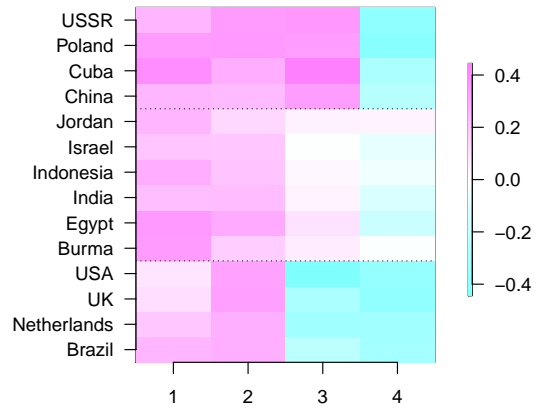
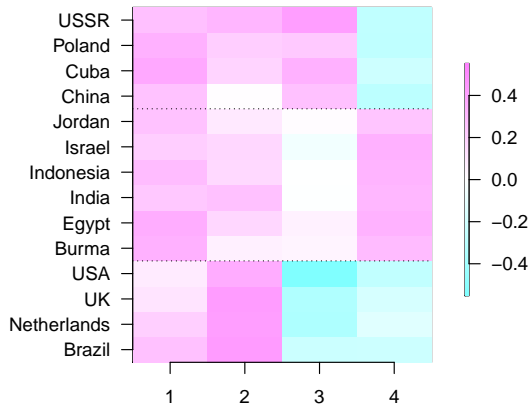


Figure 2: Heatmap of the estimated nation factors from the un-regularized model (left) and regularized model (right).

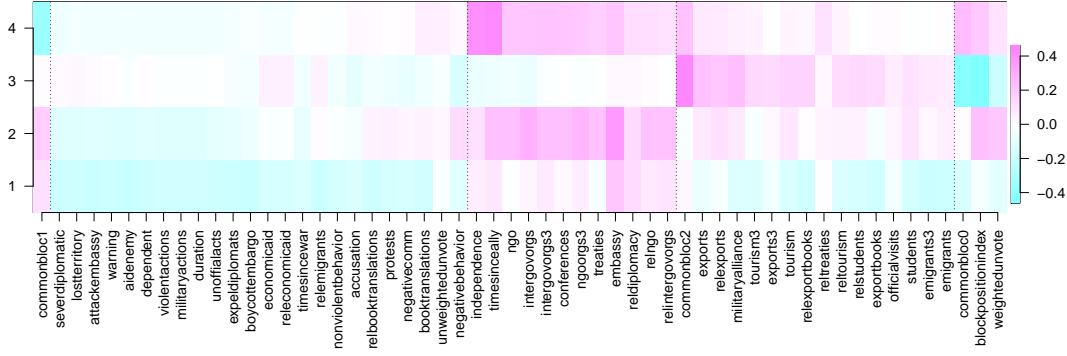


Figure 3: Heatmap of the estimated relation factors without regularization.

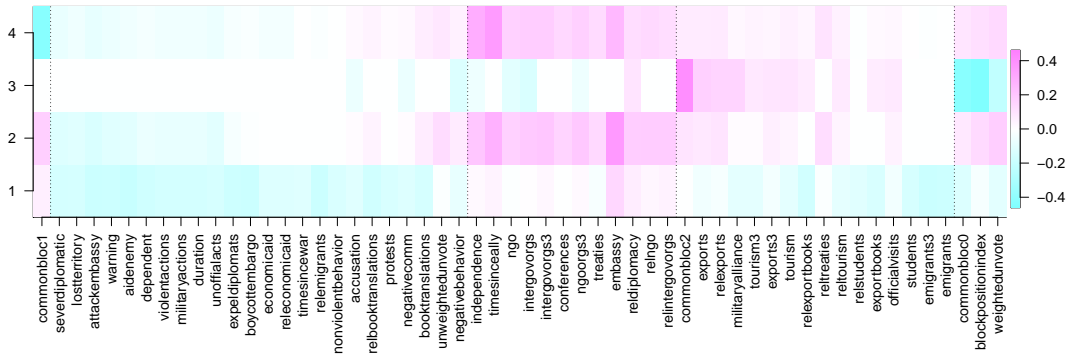


Figure 4: Heatmap of the estimated relation factors with regularization.

8.2 Co-clustering of Nations and Relations

The two-way clustering methods in Lee et al. (2010a) and Lee and Huang (2014) have been proven to be successful for analysis of continuous and binary matrix data. The core idea of two-way clustering is imposing sparsity inducing penalties on the row score vector \mathbf{u}_r and column loading vector \mathbf{v}_r in the SVD of centered data matrix or centered logit parameter matrix. This could yield a checkerboard-like structure for each rank-one matrix $d_r \cdot \mathbf{u}_r \circ \mathbf{v}_r$ for $r \in [R]$. By penalizing \mathbf{u}_r and \mathbf{v}_r in the r th component, the rows with nonzero u_{ir} are naturally clustered together, and the columns with nonzero v_{jr} are naturally clustered together. So penalization on both the score and loading vectors could simultaneously link sets of rows and sets of columns together, and reveal some desirable row-column association.

More generally, co-clustering methods could cluster related variables in each factor for tensor data. For simplicity of explanation, we focus on the three-way clustering and assume \mathbf{u}_r , \mathbf{v}_r and \mathbf{w}_r are the factors in the CP decomposition. If \mathbf{u}_r , \mathbf{v}_r and \mathbf{w}_r are sparse in the r th component, then the non-zero entries in $d_r \cdot \mathbf{u}_r \circ \mathbf{v}_r \circ \mathbf{w}_r$ form a sub-tensor for co-clustering, which could help to identify checkerboard-like local patterns of different modes. It's worth noting that different components may identify different co-clusters, and the identified co-clusters may overlap. If at least one of \mathbf{u}_r , \mathbf{v}_r and \mathbf{w}_r has the same sign in the r th component, then this component is viewed as a global pattern or a main effect. For continuous tensor data, Allen (2012) applied the sparse CP decomposition in clustering multi-way microarray data. For the analysis of the nations data, we could apply our methods for clustering associated nations and relations.

The heatmap for the estimated nation factors is displayed in the left panel of Figure 2. It doesn't have a sparse pattern. By contrast, the heatmap for the relation factors in Figure 3 does suggest a potential benefit of sparsity because many entries are close to zero. Therefore we fit a rank-4 sparse logistic CP decomposition with an ℓ_0 -norm constraint on the relation factors W . More specifically, this model imposes the constraints $\mathbf{u}_r = \mathbf{v}_r$ and $\|\mathbf{w}_r\|_0 \leq s_{3r}$, where tuning parameters s_{3r} control the number of nonzero entries in \mathbf{w}_r for $r \in [R]$. The sparse estimated relation factors are presented in Figure 4, where the nonzero entries reveal important relations in each component.

Based on the estimated nation factors \mathbf{u}_r and relation factors \mathbf{w}_r , we could build rank-one tensors $d_r \cdot \mathbf{u}_r \circ \mathbf{v}_r \circ \mathbf{w}_r$ for $r \in [R]$. For visualization, we display rank-one matrices $d_r \cdot \mathbf{u}_r \circ \mathbf{w}_r$ for $r \in [R]$. With given $r \in [R]$, \mathbf{u}_r and \mathbf{w}_r split the nations and relations into two or three clusters according to the sign of the entries, and therefore produce the clusters of nations and relations.

Figure 5 shows the heatmap of $d_r \cdot \mathbf{u}_r \circ \mathbf{w}_r$ for component 3. In the heatmap, the entries of \mathbf{u}_r and \mathbf{w}_r are arranged in increasing order. For the x -axis of the heatmap, factor \mathbf{w}_r is displayed with entries in increasing order from left to right. For the y -axis of the heatmap, factor \mathbf{u}_r is displayed with entries in increasing order from bottom to top.

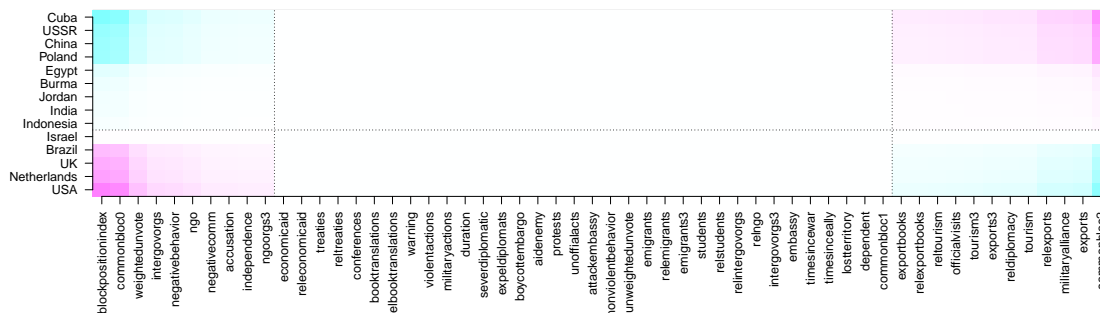


Figure 5: Heatmap of relation versus nation for component 3 with regularization.

For component 3 shown in Figure 5, negative values of the relation factor are associated with opposing common bloc membership, and positive values are associated with common bloc membership and resulting economic and cultural relations through exports and tourism. The nations are clearly separated into three groups. The nations with positive values are countries in the Communist bloc, and the nations with negative values are countries in the Western bloc. Neutral countries have almost zero values. We may as well consider imposing sparsity on this nations factor. As a form of interaction between nations and political relations, this component captures opposite political interactions between communist and western countries. It reveals a natural partition of the countries and clustering of relations as shown in Figure 5. This co-clustering suggested by the component is sensible, and the countries in the same cluster tend to share similar relation patterns.

While component 3 reflects a strong interaction between nations and political relations, the first two components mostly indicate main effects of the relations. The heatmaps of other components can be found in Appendix D.

9 Conclusions and Discussion

In this paper, we have proposed several novel tensor decomposition methods for binary tensor data using the CP decomposition of a logit parameter tensor. We have mainly focused on three-way tensors in the paper, but similar methods can be developed for higher-order data. Starting with

logistic CP decomposition, we have incorporated an ℓ_1 -norm or ℓ_0 -norm constraint on factors into the tensor decomposition formulation. To estimate factor matrices in logistic CP decomposition, we have developed computational algorithms that combine MM algorithm and variants of tensor power method. By imposing sparsity constraints on the factor matrices, we could identify and select important features in each factor. Sparse logistic CP decompositions can capture local multi-way interactions and therefore facilitate co-clustering of entities in different modes. Such co-clusters can reveal interesting associations between different modes.

There are several directions worth further investigation. As a structural element in logistic tensor decomposition, we have considered a constant offset term only. However, main effects along each mode are likely to be significant systematic elements in many applications as evidenced in the nations data analysis as well. From a modeling point of view, including additive main effects in the decomposition and using a small number of sparse rank-one tensors for multiplicative interactions will be a fruitful direction for extension. A similar logistic ANOVA model has been proposed for binary matrix data (Jung et al., 2014).

As another extension, we could generalize the current formulation with CP decomposition for binary data to a Tucker decomposition and develop a corresponding regularized version. Besides, we could replace the ℓ_0 -norm and ℓ_1 -norm penalties with general penalties such as fused lasso (Tibshirani et al., 2005) in certain applications. For example, when one mode of a given tensor represents time points, smoothness in temporal factors might be desired.

Throughout the paper we only discuss the logit link function for binary data, but we could also develop logistic CP decompositions with the probit link function (i.e., $\theta = \Phi^{-1}(p)$ using the cdf of standard normal distribution Φ). Similar to the logit link, we can use the quadratic majorization of $-\log \Phi(x)$ from de Leeuw (2006) to devise MM algorithms.

On the theoretical front, it is of interest to extend the work of Montanari and Richard (2014) to binary tensors and investigate conditions on the signal-to-noise ratio to recover true factor matrices from an observed binary tensor with high probability. Moreover, the optimality of model selection approaches in binary tensor decomposition is still unknown, and it is worth investigating the consistency of AIC, BIC or other information criteria.

Last but not least, we could develop similar methods for tensor decompositions in the natural parameter space for other types of exponential family data. For example, tensor data with counts or ratings as entries are common in recommender systems. Sparse Poisson or multinomial CP decompositions will be useful extensions of the current work.

Acknowledgments

This research was supported in part by the National Science Foundation Grants DMS-15-13566 and DMS-20-15490.

References

- Acar, E., Dunlavy, D. M., Kolda, T. G., and Mørup, M. (2011). Scalable tensor factorizations for incomplete data. *Chemometrics and Intelligent Laboratory Systems*, 106(1):41–56.
- Allen, G. (2012). Sparse higher-order principal components analysis. In *Artificial Intelligence and Statistics*, pages 27–36.
- Anandkumar, A., Ge, R., and Janzamin, M. (2014). Guaranteed non-orthogonal tensor decomposition via alternating rank-1 updates. *arXiv preprint arXiv:1402.5180*.

- Bi, X., Qu, A., and Shen, X. (2018). Multilayer tensor factorization with applications to recommender systems. *The Annals of Statistics*, 46(6B):3308–3333.
- Boyd, S. and Vandenberghe, L. (2004). *Convex Optimization*. Cambridge University Press.
- Bro, R. (1997). PARAFAC. Tutorial and applications. *Chemometrics and Intelligent Laboratory Systems*, 38(2):149–171.
- Carroll, J. D. and Chang, J.-J. (1970). Analysis of individual differences in multidimensional scaling via an n-way generalization of “Eckart-Young” decomposition. *Psychometrika*, 35(3):283–319.
- Collins, M., Dasgupta, S., and Schapire, R. E. (2002). A generalization of principal components analysis to the exponential family. In *Advances in Neural Information Processing Systems*, pages 617–624.
- de Leeuw, J. (2006). Principal component analysis of binary data by iterated singular value decomposition. *Computational Statistics & Data Analysis*, 50(1):21 – 39. 2nd Special issue on Matrix Computations and Statistics.
- Golub, G. H. and van Loan, C. F. (1996). *Matrix Computations*. The Johns Hopkins University Press, Baltimore, USA.
- Harshman, R. (1970). Foundations of the PARAFAC procedure: Models and conditions for an “explanatory” multimodal factor analysis. *UCLA Working Papers in Phonetics*, 16:1–84.
- Hong, D., Kolda, T. G., and Duersch, J. A. (2020). Generalized canonical polyadic tensor decomposition. *SIAM Review*, 62(1):133–163.
- Hunter, D. R. and Lange, K. (2004). A tutorial on MM algorithms. *The American Statistician*, 58(1):30–37.
- Jaakkola, T. S. and Jordan, M. I. (2000). Bayesian parameter estimation via variational methods. *Statistics and Computing*, 10(1):25–37.
- Jolliffe, I. T., Trendafilov, N. T., and Uddin, M. (2003). A modified principal component technique based on the lasso. *Journal of Computational and Graphical Statistics*, 12(3):531–547.
- Jung, Y., Huang, J. Z., and Hu, J. (2014). Biomarker detection in association studies: modeling snps simultaneously via logistic anova. *Journal of the American Statistical Association*, 109(508):1355–1367.
- Kemp, C., Tenenbaum, J. B., Griffiths, T. L., Yamada, T., and Ueda, N. (2006). Learning systems of concepts with an infinite relational model. In *AAAI*, volume 3, page 5.
- Kolda, T. G. and Bader, B. W. (2009). Tensor decompositions and applications. *SIAM Review*, 51(3):455–500.
- Kruskal, J. B. (1977). Three-way arrays: rank and uniqueness of trilinear decompositions, with application to arithmetic complexity and statistics. *Linear Algebra and its Applications*, 18(2):95–138.
- Kruskal, J. B. (1989). Rank, decomposition, and uniqueness for 3-way and N -way arrays. *Multivariate Data Analysis*, pages 7–18.

- Landgraf, A. J. and Lee, Y. (2020a). Dimensionality reduction for binary data through the projection of natural parameters. *Journal of Multivariate Analysis*, 180:104668.
- Landgraf, A. J. and Lee, Y. (2020b). Generalized principal component analysis: Projection of saturated model parameters. *Technometrics*, 62(4):459–472.
- Lee, M., Shen, H., Huang, J. Z., and Marron, J. (2010a). Biclustering via sparse singular value decomposition. *Biometrics*, 66(4):1087–1095.
- Lee, S. and Huang, J. Z. (2014). A biclustering algorithm for binary matrices based on penalized Bernoulli likelihood. *Statistics and Computing*, 24(3):429–441.
- Lee, S., Huang, J. Z., and Hu, J. (2010b). Sparse logistic principal components analysis for binary data. *The Annals of Applied Statistics*, 4(3):1579.
- Li, G. (2020). Generalized co-clustering analysis via regularized alternating least squares. *Computational Statistics & Data Analysis*, page 106989.
- Li, J., Bien, J., and Wells, M. T. (2018). rTensor: An R package for multidimensional array (tensor) unfolding, multiplication, and decomposition. *Journal of Statistical Software*, 87(10):1–31.
- Lloyd, S. (1982). Least squares quantization in PCM. *IEEE Transactions on Information Theory*, 28(2):129–137.
- MacQueen, J. (1967). Some methods for classification and analysis of multivariate observations. In *Proceedings of the Fifth Berkeley Symposium on Mathematical Statistics and Probability*, volume 1, pages 281–297. Oakland, CA, USA.
- Madrid-Padilla, O. H. and Scott, J. (2017). Tensor decomposition with generalized lasso penalties. *Journal of Computational and Graphical Statistics*, 26(3):537–546.
- Mažgut, J., Tiño, P., Bodén, M., and Yan, H. (2014). Dimensionality reduction and topographic mapping of binary tensors. *Pattern Analysis and Applications*, 17(3):497–515.
- Montanari, A. and Richard, E. (2014). A statistical model for tensor PCA. In *Advances in Neural Information Processing Systems*, pages 2897–2905.
- Nickel, M., Tresp, V., and Kriegel, H.-P. (2011). A three-way model for collective learning on multi-relational data. In *Proceedings of the 28th International Conference on Machine Learning*, pages 809–816.
- R Core Team (2019). *R: A Language and Environment for Statistical Computing*. R Foundation for Statistical Computing, Vienna, Austria.
- Rummel, R. J. (1968). Dimensionality of nations project. Technical report, Department of Political Science, Hawaii University, Honolulu.
- Shen, H. and Huang, J. Z. (2008). Sparse principal component analysis via regularized low rank matrix approximation. *Journal of Multivariate Analysis*, 99(6):1015–1034.
- Shi, C., Lu, W., and Song, R. (2019). Determining the number of latent factors in statistical multi-relational learning. *The Journal of Machine Learning Research*, 20(1):809–846.

- Sun, W. W., Lu, J., Liu, H., and Cheng, G. (2017). Provable sparse tensor decomposition. *Journal of the Royal Statistical Society: Series B (Statistical Methodology)*, 79(3):899–916.
- Tibshirani, R., Saunders, M., Rosset, S., Zhu, J., and Knight, K. (2005). Sparsity and smoothness via the fused lasso. *Journal of the Royal Statistical Society: Series B (Statistical Methodology)*, 67(1):91–108.
- Tucker, L. R. (1966). Some mathematical notes on three-mode factor analysis. *Psychometrika*, 31(3):279–311.
- Udell, M., Horn, C., Zadeh, R., and Boyd, S. (2016). Generalized low rank models. *Foundations and Trends® in Machine Learning*, 9(1):1–118.
- Wang, M., Fischer, J., and Song, Y. S. (2019). Three-way clustering of multi-tissue multi-individual gene expression data using semi-nonnegative tensor decomposition. *The Annals of Applied Statistics*, 13(2):1103–1127.
- Wang, M. and Li, L. (2020). Learning from binary multiway data: Probabilistic tensor decomposition and its statistical optimality. *Journal of Machine Learning Research*, 21(154):1–38.
- Witten, D. M., Tibshirani, R., and Hastie, T. (2009). A penalized matrix decomposition, with applications to sparse principal components and canonical correlation analysis. *Biostatistics*, 10(3):515–534.
- Yuan, X.-T. and Zhang, T. (2013). Truncated power method for sparse eigenvalue problems. *Journal of Machine Learning Research*, 14(Apr):899–925.
- Zhang, A. and Han, R. (2019). Optimal sparse singular value decomposition for high-dimensional high-order data. *Journal of the American Statistical Association*, 114(528):1708–1725.
- Zhou, H., Li, L., and Zhu, H. (2013). Tensor regression with applications in neuroimaging data analysis. *Journal of the American Statistical Association*, 108(502):540–552.
- Zou, H., Hastie, T., and Tibshirani, R. (2006). Sparse principal component analysis. *Journal of Computational and Graphical Statistics*, 15(2):265–286.

Appendix

A Algorithms

We summarize the proposed algorithms for logistic tensor decomposition with alternating least squares method, tensor soft-thresholding power method and tensor truncated power method in Algorithms 2, 3 and 4.

Algorithm 2 MM-Alternating Least Squares algorithm for logistic CP decomposition

- 1: **input:** tensor \mathcal{X} and rank R .
 - 2: Initialize with $\hat{\mu}^{[0]}$ and $(\hat{\mathbf{d}}^{[0]}, \hat{U}^{[0]}, \hat{V}^{[0]}, \hat{W}^{[0]})$. Set $m = 0$.
 - 3: **repeat**
 - 4: Compute $\mathcal{Z}^{[m]}$ in (3).
 - 5: Update $\hat{\mu}^{[m+1]}$.
 - 6: Compute $\mathcal{Z}_c^{[m]} = \mathcal{Z}^{[m]} - \hat{\mu}^{[m+1]} \mathbf{1}_{p_1 p_2 p_3}$.
 - 7: Initialize with $(\hat{\mathbf{d}}^{[m]}, \hat{U}^{[m]}, \hat{V}^{[m]}, \hat{W}^{[m]})$.
 - 8: **repeat**
 - 9: $U \leftarrow \text{Normalize}(\mathcal{Z}_{c(1)}^{[m]} [(W \odot V)^T]^\dagger)$
 - 10: $V \leftarrow \text{Normalize}(\mathcal{Z}_{c(2)}^{[m]} [(U \odot W)^T]^\dagger)$
 - 11: $W \leftarrow \text{Normalize}(\mathcal{Z}_{c(3)}^{[m]} [(U \odot V)^T]^\dagger)$.
 - 12: $\mathbf{d} \leftarrow$ column norms of $\mathcal{Z}_{c(3)}^{[m]} [(U \odot V)^T]^\dagger$
 - 13: **until** converge
 - 14: Update $(\hat{\mathbf{d}}^{[m+1]}, \hat{U}^{[m+1]}, \hat{V}^{[m+1]}, \hat{W}^{[m+1]})$.
 - 15: $m \leftarrow m + 1$
 - 16: **until** converge
 - 17: **output:** $\hat{\mu}$ and $(\hat{\mathbf{d}}, \hat{U}, \hat{V}, \hat{W})$.
-

Algorithm 3 MM-Tensor Soft-thresholding Power algorithm for sparse logistic CP decomposition

- 1: **input:** tensor \mathcal{X} , number of initializations L , rank R , and penalization vector (c_1, c_2, c_3) .
 - 2: Initialize with $\hat{\mu}_\tau^{[0]}$ and $(\hat{\mathbf{u}}_\tau^{[0]}, \hat{\mathbf{v}}_\tau^{[0]}, \hat{\mathbf{w}}_\tau^{[0]})$ where $\tau \in [L]$. Set $m = 0$.
 - 3: **for** $\tau = 1$ **to** L **do**
 - 4: **repeat**
 - 5: Compute $\mathcal{Z}^{[m]}$ in (3).
 - 6: Update $\hat{\mu}^{[m+1]}$.
 - 7: Compute $\mathcal{Z}_c^{[m]} = \mathcal{Z}^{[m]} - \hat{\mu}^{[m+1]} \mathbf{1}_{p_1 p_2 p_3}$.
 - 8: **repeat**
 - 9: $\mathbf{u}_\tau = \text{Normalize}(S(\mathcal{Z}_c^{[m]} \times_2 (\mathbf{v}_\tau)^T \times_3 (\mathbf{w}_\tau)^T, \lambda_1))$
 - 10: $\mathbf{v}_\tau = \text{Normalize}(S(\mathcal{Z}_c^{[m]} \times_1 (\mathbf{u}_\tau)^T \times_3 (\mathbf{w}_\tau)^T, \lambda_2))$
 - 11: $\mathbf{w}_\tau = \text{Normalize}(S(\mathcal{Z}_c^{[m]} \times_1 (\mathbf{u}_\tau)^T \times_2 (\mathbf{v}_\tau)^T, \lambda_3))$
 - 12: **until** converge
 - 13: Update $(\hat{\mathbf{d}}_\tau^{[m+1]}, \hat{\mathbf{u}}_\tau^{[m+1]}, \hat{\mathbf{v}}_\tau^{[m+1]}, \hat{\mathbf{w}}_\tau^{[m+1]})$.
 - 14: $m \leftarrow m + 1$
 - 15: **until** converge
 - 16: Return $\hat{\mu}_\tau$ and $(\hat{\mathbf{d}}_\tau, \hat{\mathbf{u}}_\tau, \hat{\mathbf{v}}_\tau, \hat{\mathbf{w}}_\tau)$.
 - 17: **end for**
 - 18: Cluster $\{(\hat{\mathbf{d}}_\tau, \hat{\mathbf{u}}_\tau, \hat{\mathbf{v}}_\tau, \hat{\mathbf{w}}_\tau), \tau \in [L]\}$ into R clusters $\{(\hat{\mathbf{d}}_j, \hat{\mathbf{u}}_j, \hat{\mathbf{v}}_j, \hat{\mathbf{w}}_j), j \in [R]\}$ by Algorithm 5.
 - 19: **output:** $\hat{\mu}$ and R clusters $\{(\hat{\mathbf{d}}_j, \hat{\mathbf{u}}_j, \hat{\mathbf{v}}_j, \hat{\mathbf{w}}_j), j \in [R]\}$.
-

Algorithm 4 MM-Tensor Truncated Power algorithm for sparse logistic CP decomposition

- 1: **input:** tensor \mathcal{X} , number of initializations L , rank R , and cardinality vector (s_1, s_2, s_3) .
 - 2: Initialize with $\hat{\mu}_\tau^{[0]}$ and $(\hat{\mathbf{u}}_\tau^{[0]}, \hat{\mathbf{v}}_\tau^{[0]}, \hat{\mathbf{w}}_\tau^{[0]})$ where $\tau \in [L]$. Set $m = 0$.
 - 3: **for** $\tau = 1$ **to** L **do**
 - 4: **repeat**
 - 5: Compute $\mathcal{Z}^{[m]}$ in (3).
 - 6: Update $\hat{\mu}^{[m+1]}$.
 - 7: Compute $\mathcal{Z}_c^{[m]} = \mathcal{Z}^{[m]} - \hat{\mu}^{[m+1]} \mathbf{1}_{p_1 p_2 p_3}$.
 - 8: **repeat**
 - 9: $\mathbf{u}_\tau = \text{Normalize}(T(\mathcal{Z}_c^{[m]} \times_2 (\mathbf{v}_\tau)^T \times_3 (\mathbf{w}_\tau)^T, s_1))$
 - 10: $\mathbf{v}_\tau = \text{Normalize}(T(\mathcal{Z}_c^{[m]} \times_1 (\mathbf{u}_\tau)^T \times_3 (\mathbf{w}_\tau)^T, s_2))$
 - 11: $\mathbf{w}_\tau = \text{Normalize}(T(\mathcal{Z}_c^{[m]} \times_1 (\mathbf{u}_\tau)^T \times_2 (\mathbf{v}_\tau)^T, s_3))$
 - 12: **until** converge
 - 13: Update $(\hat{d}_\tau^{[m+1]}, \hat{\mathbf{u}}_\tau^{[m+1]}, \hat{\mathbf{v}}_\tau^{[m+1]}, \hat{\mathbf{w}}_\tau^{[m+1]})$.
 - 14: $m \leftarrow m + 1$
 - 15: **until** converge
 - 16: Return $\hat{\mu}_\tau$ and $(\hat{d}_\tau, \hat{\mathbf{u}}_\tau, \hat{\mathbf{v}}_\tau, \hat{\mathbf{w}}_\tau)$.
 - 17: **end for**
 - 18: Cluster $\{(\hat{d}_\tau, \hat{\mathbf{u}}_\tau, \hat{\mathbf{v}}_\tau, \hat{\mathbf{w}}_\tau), \tau \in [L]\}$ into R clusters $\{(\hat{d}_j, \hat{\mathbf{u}}_j, \hat{\mathbf{v}}_j, \hat{\mathbf{w}}_j), j \in [R]\}$ by Algorithm 5.
 - 19: **output:** $\hat{\mu}$ and R clusters $\{(\hat{d}_j, \hat{\mathbf{u}}_j, \hat{\mathbf{v}}_j, \hat{\mathbf{w}}_j), j \in [R]\}$.
-

B Simulation Study

B.1 BIC and AIC

For illustration, we simulated binary data of size $p_1 = 1000, p_2 = 100$ and $p_3 = 10$ from a rank-2 logit tensor. Due to the sparsity in factors, the underlying logit tensor is also very sparse. The level of sparsity in each dimension is set to be equal. The details of the simulation setting can be found in Section 7.1. In this setting, we could express the tuning parameters $c_i = c\sqrt{p_i}$ or $s_i = sp_i$ using a common ratio parameter c or s . For feasibility, the ratio parameters c and s should satisfy $\max_i \frac{1}{\sqrt{p_i}} \leq c \leq 1$ and $\max_i \frac{1}{p_i} \leq s \leq 1$, respectively. Figure 6 shows how BIC and AIC change with rank R for the simulated data. It shows that AIC selects the true rank ($R = 2$) correctly while BIC chooses a smaller rank ($R = 1$). For the same data, Figures 7 and 8 show how BIC and AIC change with ratio $c \in [\max_i \frac{1}{\sqrt{p_i}}, 1]$ and ratio $s \in [\max_i \frac{1}{p_i}, 1]$ given rank $R = 2$. Clearly, regularized models have a smaller BIC/AIC than the un-regularized model, and the optimal tuning parameter can be selected by minimizing BIC and AIC. Our limited experiments suggest that AIC tends to be more accurate than BIC in selecting the rank R .

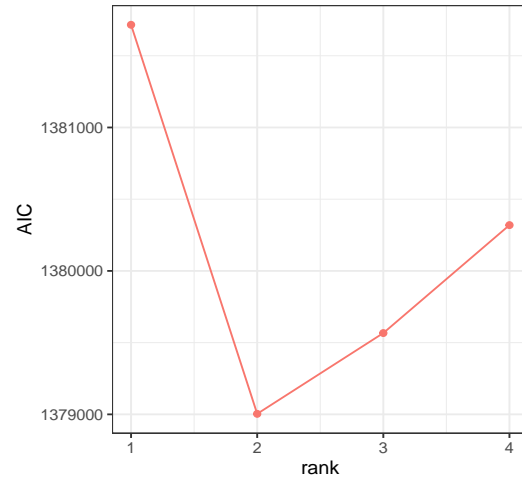
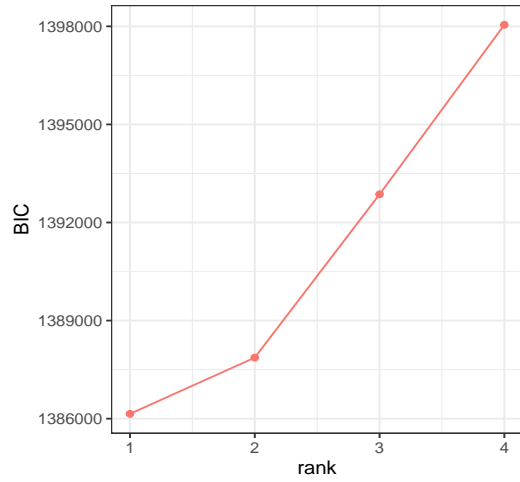


Figure 6: BIC and AIC versus rank R for simulated data with $p_1 = 1000, p_2 = 100, p_3 = 10$ and $R = 2$.

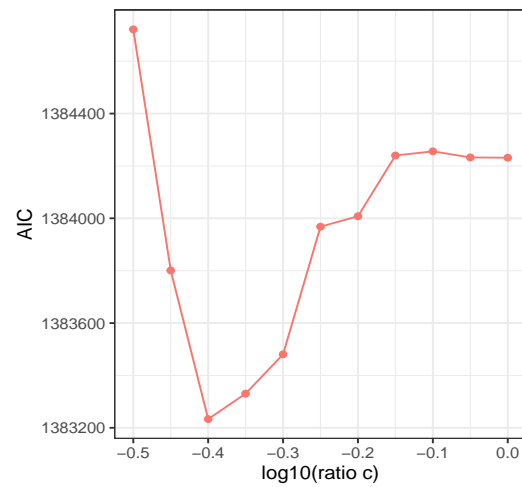
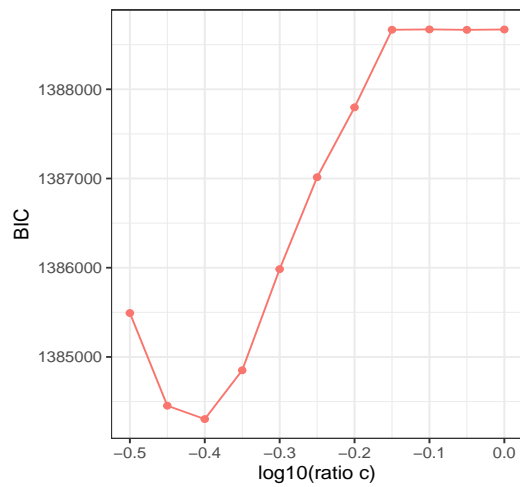


Figure 7: BIC and AIC versus ratio c when rank R is fixed at 2 for simulated data with $p_1 = 1000, p_2 = 100, p_3 = 10$ and $R = 2$.

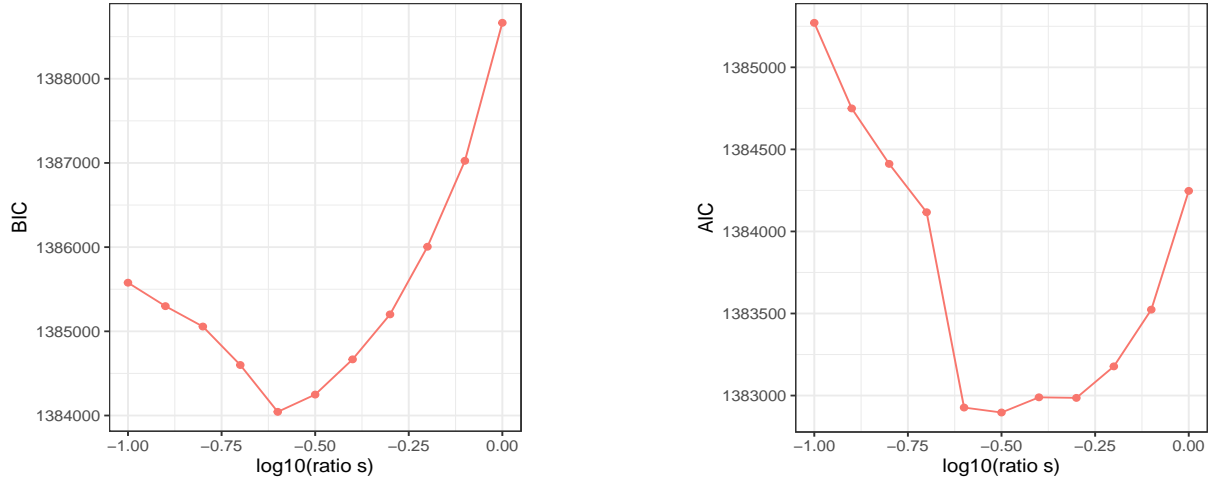


Figure 8: BIC and AIC versus ratio s when rank R is fixed at 2 for simulated data with $p_1 = 1000, p_2 = 100, p_3 = 10$ and $R = 2$.

B.2 Cross-validation

We apply cross-validation to the same simulated data used for BIC and AIC. Figures 9 and 10 show the average negative log likelihood over training data (training error) and that over test data (test error). The test error is minimized when the rank is 2. Also we find the selected ratio c and ratio s values are close to those from BIC and AIC.

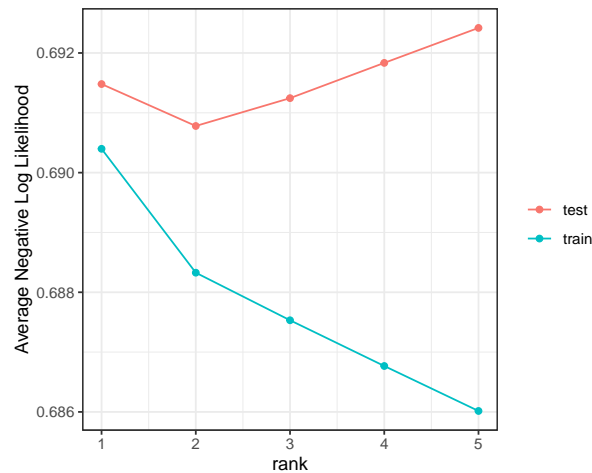


Figure 9: Training error and test error measured in terms of the average negative log likelihood versus rank R for simulated data with $p_1 = 1000, p_2 = 100, p_3 = 10$ and $R = 2$.

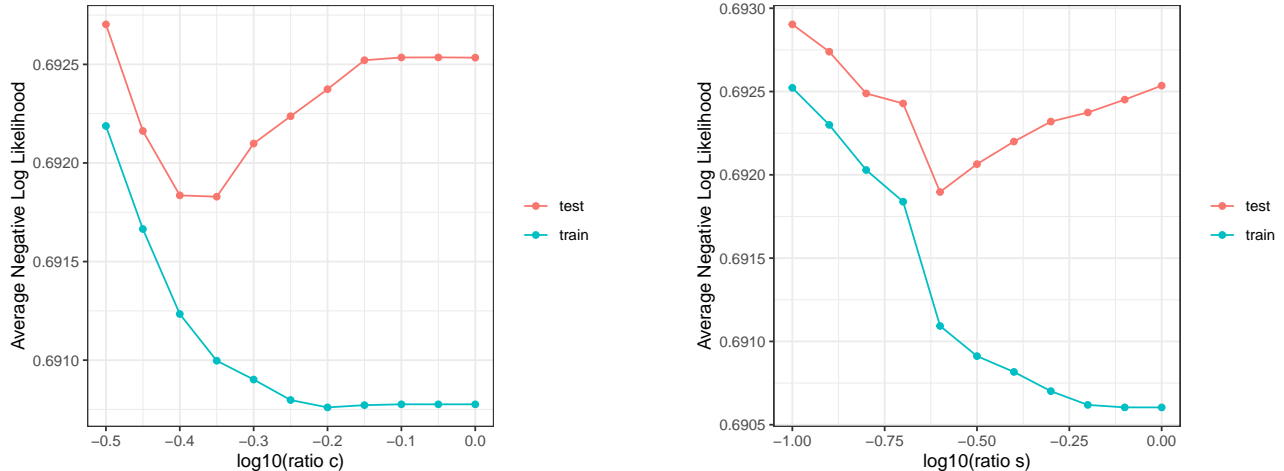


Figure 10: Training error and test error measured in terms of the average negative log likelihood versus ratio c (left) and ratio s (right) for simulated data with $p_1 = 1000, p_2 = 100, p_3 = 10$ and $R = 2$.

B.3 Explained Deviance

In general, there is a tradeoff between the sparsity of factor matrices and the explained deviance. We illustrate the tradeoff using the simulated data as before. Here we fit ℓ_1 -norm and ℓ_0 -norm regularized rank-two models with varying tuning parameter values c and s , respectively. When ratio $c \in [\max_i \frac{1}{\sqrt{p_i}}, 1]$ or ratio $s \in [\max_i \frac{1}{p_i}, 1]$ decreases, the factor matrices become sparser and easier to interpret. However, as shown in Figure 11, the cumulative percentage of explained deviance for the first two components and marginal percentage of explained deviance of the first component and second component also tend to be smaller compared to the un-regularized model. Besides, we fit a rank-five model with all methods including ALS and TP for logistic CP decomposition, ℓ_0 -TP and ℓ_1 -TP for sparse logistic CP decomposition. The cumulative percentage of explained deviance by the first 5 components is shown in Figure 12. The percentage is small due to the sparsity in Θ . For comparison, we consider a subset $\Omega = \{(i, j, k) : \theta_{ijk}^* \neq 0\}$, and calculate the explained deviance based on the partial data \mathcal{X}_Ω with nonzero θ_{ijk}^* only. The cumulative percentages of deviance explained by the five components based on \mathcal{X}_Ω are 26.62, 45.05, 45.08, 45.17 and 45.17. The marginal percentages of deviance explained by each of the five components are 26.62, 18.43, 0.035, 0.085 and 0.0019. We find that the explained deviance for the partial data is much higher than the whole data. It's clear that TP method and ALS method produce a very close explained deviance. The same is true for TSP method and TTP method, but their solutions explain less deviance due to the sparsity in factors. As in standard PCA, a scree plot of marginal explained deviance can be used to determine the number of rank and degree of sparsity for tensor decomposition. The left panel of Figure 12 indicates an elbow point around $R = 3$ and suggests the choice of rank 2, which is the same as the true rank.

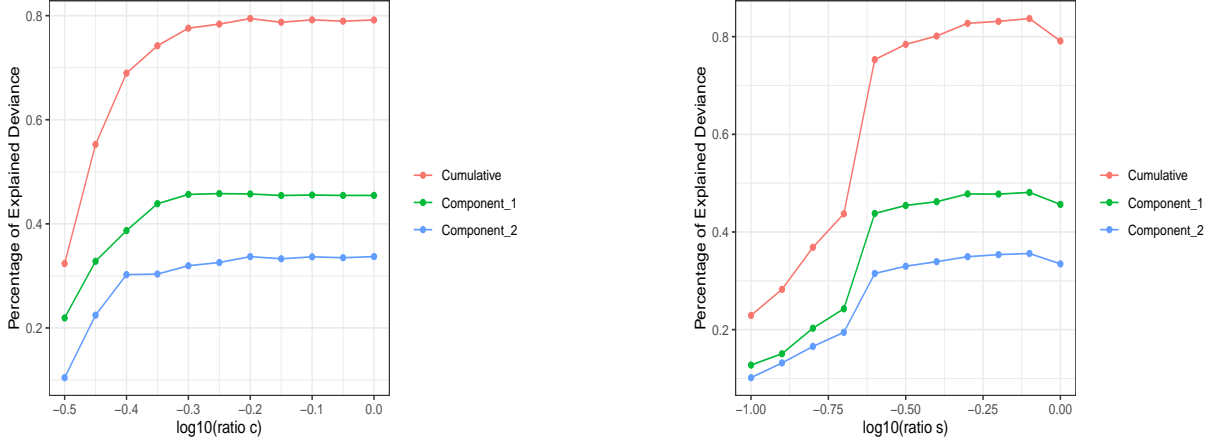


Figure 11: The percentage of the deviance explained by the first two components in sparse logistic tensor decomposition constrained with ℓ_1 -norm (left) and ℓ_0 -norm (right) for simulated data with $p_1 = 1000, p_2 = 100, p_3 = 10$ and $R = 2$.

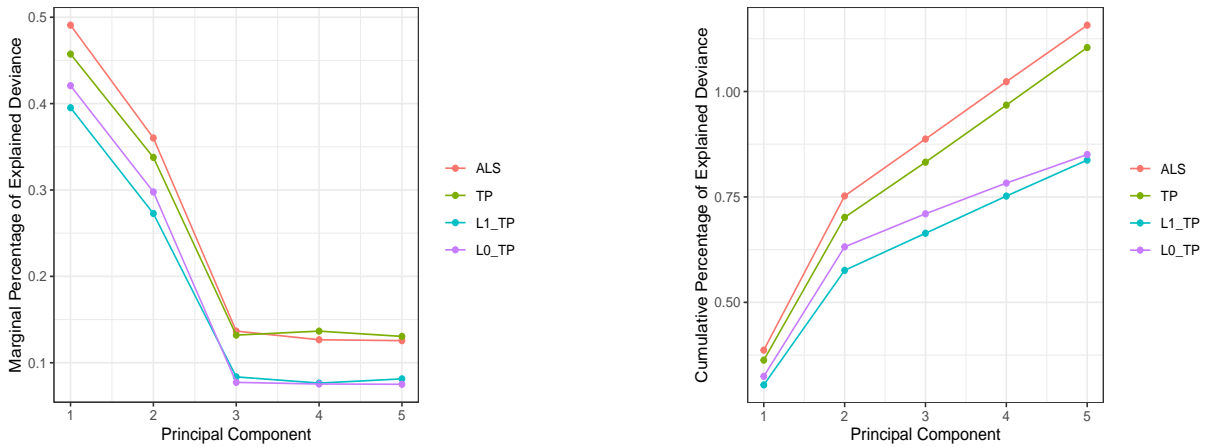


Figure 12: The percentage of explained deviance in logistic tensor decomposition by four methods for simulated data with $p_1 = 1000, p_2 = 100, p_3 = 10$ and $R = 2$. The marginal percentage of deviance explained by each of the five components (left) and the cumulative percentage of deviance explained by the five components (right).

B.4 True Positive Rate and False Positive Rate

Figure 13 shows how the mean TPR and FPR change with ratio $c \in [\max_i \frac{1}{p_i}, 1]$ and ratio $s \in [\max_i \frac{1}{p_i}, 1]$ for simulated data from scenario 4. Both ℓ_1 -norm and ℓ_0 -norm penalties can do selection of nonzero parameters in sparse logistic CP decomposition. The receiver operating characteristic (ROC) curves for both methods in Figure 14 show that they have comparable area under the curve (AUC) values. Results are similar for other settings and thus omitted.

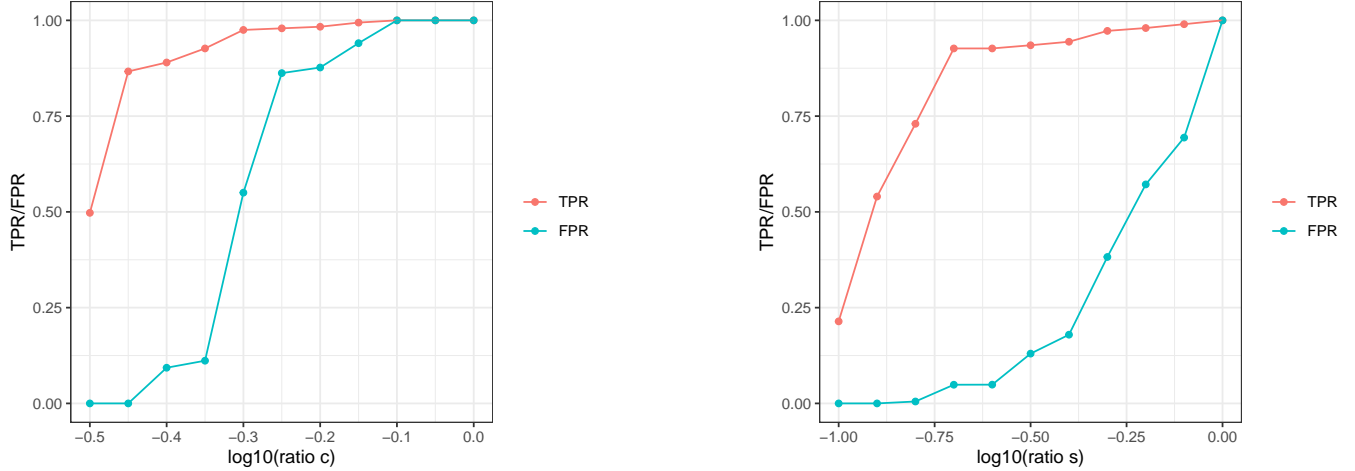


Figure 13: TPR and FPR in ℓ_1 -norm constrained logistic tensor decomposition with ratio c (left), and ℓ_0 -norm constrained decomposition with ratio s (right) for simulated data with $p_1 = 1000, p_2 = 10, p_3 = 10$ and $R = 2$.

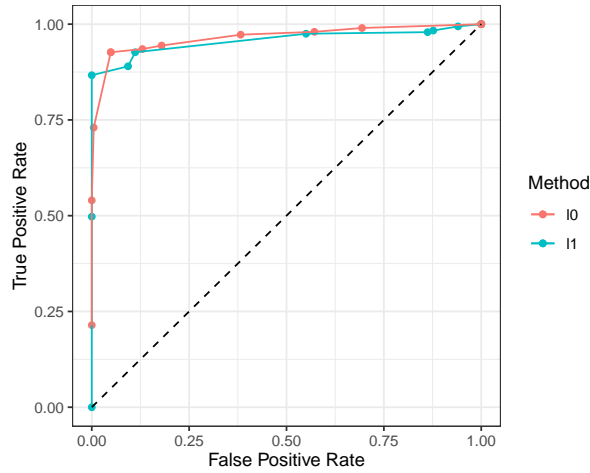


Figure 14: ROC curves of ℓ_1 -norm constrained logistic tensor decomposition and ℓ_0 -norm constrained decomposition for simulated data with $p_1 = 1000, p_2 = 10, p_3 = 10$ and $R = 2$.

B.5 Estimation Errors

To illustrate the benefit of regularization, we generate data from scenario 3 and show the RMSE and Mean Error of ℓ_1 -norm and ℓ_0 -norm constrained logistic tensor decompositions, respectively, as a function of the ratio parameter in Figure 16. Clearly, ℓ_1 -norm and ℓ_0 -norm regularizations help to reduce both the overall estimation error and component estimation error if the true factors are sparse. Note that the estimation errors for un-regularized solutions at $c = 1$ and $s = 1$ differ slightly due to difference in initializations.

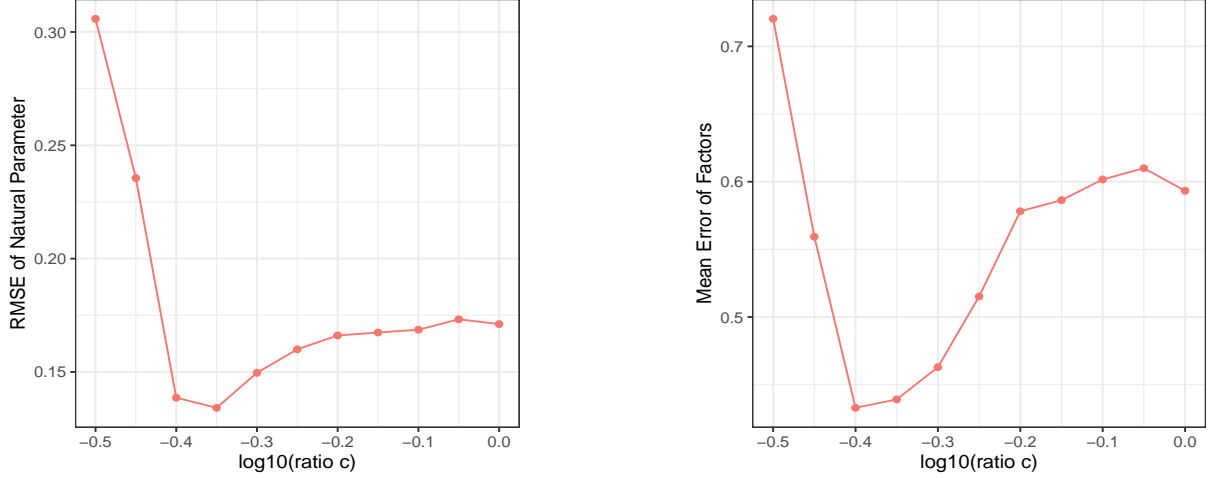


Figure 15: RMSE and mean error in ℓ_1 -norm constrained logistic tensor decomposition with ratio c for simulated data from scenario 3.

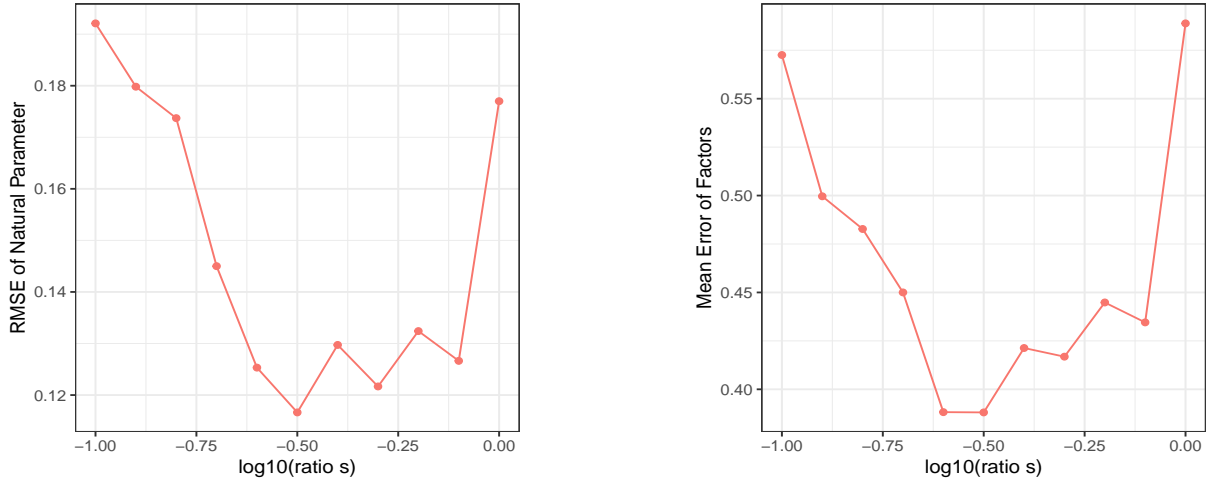


Figure 16: RMSE and mean error in ℓ_0 -norm constrained logistic tensor decomposition with ratio s for simulated data from scenario 3.

C Choice of Parameters in Algorithms

In order to obtain accurate estimates of logit parameters, we need to choose control parameters in algorithms carefully in practice. In this section, we discuss the initialization and termination of the proposed algorithms as well as the clustering procedure.

C.1 Initialization

There are two kinds of initialization for the proposed algorithms: one is spectral initialization and the other is random initialization. For Alternating Least Squares (ALS) method, *spectral initialization* starts with the tensor $2\mathcal{X} - \mathbf{1}_{p_1 p_2 p_3}$, and obtains $\mu = \frac{1}{p_1 p_2 p_3} (2\mathcal{X} - \mathbf{1}_{p_1 p_2 p_3}) \times_1 \mathbf{1}_{p_1}^T \times_2 \mathbf{1}_{p_2}^T \times_3 \mathbf{1}_{p_3}^T$ and $\mathcal{Q} = (2\mathcal{X} - \mathbf{1}_{p_1 p_2 p_3}) - \mu \mathbf{1}_{p_1 p_2 p_3}$. Then it extracts the left R singular vectors of

matricizations of \mathcal{Q} , say $Q_{(1)}$ and $Q_{(2)}$ as the initialization of factor matrices U and V , and lets $W = Q_{(3)}[(U \odot V)^T]^{-1}$. *Random initialization* starts with matrices U and V where their entries are independently generated from the standard Gaussian distribution. Then it normalizes the matrices U and V to those with unit columns and lets $W = Q_{(3)}[(U \odot V)^T]^{-1}$. With μ, U, V and W , we could define $\Theta^{[0]}$ using (1) and then $\mathcal{Z}^{[0]}$ using (3).

For Tensor Power (TP) method, *spectral initialization* of a rank-one model first generates $\theta \sim N(0, I_{p_3})$, and truncates θ to $\theta' = T(\theta, \max\{s_1, s_2, s_3\})$. Then it calculates $\mathbf{u} \in \mathbb{R}^{p_1}$ and $\mathbf{v} \in \mathbb{R}^{p_2}$ as the leading left and right singular vectors of $\mathcal{Q} \times_3 (\theta')^T \in \mathbb{R}^{p_1 \times p_2}$. Finally it computes sparse vectors $\mathbf{u}' = T(\mathbf{u}, s_1)$ and $\mathbf{v}' = T(\mathbf{v}, s_2)$, normalizes them by $\bar{\mathbf{u}} = \mathbf{u}'/\|\mathbf{u}'\|_2$ and $\bar{\mathbf{v}} = \mathbf{v}'/\|\mathbf{v}'\|_2$ and calculates $\bar{\mathbf{w}} = \mathcal{Q} \times_1 \bar{\mathbf{u}}^T \times_2 \bar{\mathbf{v}}^T \in \mathbb{R}^{p_3}$. $(\bar{\mathbf{u}}, \bar{\mathbf{v}}, \bar{\mathbf{w}})$ is the initial value from this spectral initialization. On the other hand, *random initialization* of a rank-one model first generates $\mathbf{u} \sim N(0, I_{p_1})$ and $\mathbf{v} \sim N(0, I_{p_2})$, and then computes the sparse vectors $\mathbf{u}' = T(\mathbf{u}, s_1)$ and $\mathbf{v}' = T(\mathbf{v}, s_2)$. Then it normalizes them by $\bar{\mathbf{u}} = \mathbf{u}'/\|\mathbf{u}'\|_2$ and $\bar{\mathbf{v}} = \mathbf{v}'/\|\mathbf{v}'\|_2$, and finally calculates $\bar{\mathbf{w}} = \mathcal{Q} \times_1 \bar{\mathbf{u}}^T \times_2 \bar{\mathbf{v}}^T \in \mathbb{R}^{p_3}$. This gives $(\bar{\mathbf{u}}, \bar{\mathbf{v}}, \bar{\mathbf{w}})$ as the initial value. With $\mu, \bar{\mathbf{u}}, \bar{\mathbf{v}}$ and $\bar{\mathbf{w}}$, we could define $\Theta^{[0]}$ and $\mathcal{Z}^{[0]}$ using (7) and (3).

Overall, the above initializations are based on a fully observed data tensor. In practice, if the input data tensor \mathcal{X} contains missing values, we could set all missing entries of \mathcal{X} to 1/2, or equivalently set all missing entries of $2\mathcal{X} - \mathbf{1}_{p_1 p_2 p_3}$ to zero.

C.2 Termination

For the tensor power methods in Algorithms 1, 3 and 4, we terminate the inner loop when

$$\max\{\|\hat{\mathbf{u}}_\tau^{[n+1]} - \hat{\mathbf{u}}_\tau^{[n]}\|_2, \|\hat{\mathbf{v}}_\tau^{[n+1]} - \hat{\mathbf{v}}_\tau^{[n]}\|_2, \|\hat{\mathbf{w}}_\tau^{[n+1]} - \hat{\mathbf{w}}_\tau^{[n]}\|_2\} \leq 10^{-4}$$

is satisfied for some iteration n . For the alternating least squares method in Algorithm 2 with rank R , we terminate the inner loop when

$$\max\{\|\hat{U}^{[n+1]} - \hat{U}^{[n]}\|_F, \|\hat{V}^{[n+1]} - \hat{V}^{[n]}\|_F, \|\hat{W}^{[n+1]} - \hat{W}^{[n]}\|_F\} \leq \sqrt{R} \cdot 10^{-4}$$

is satisfied for some iteration n .

For the outer loop (MM algorithm) of Algorithms 2, 1, 3 and 4, the maximal number of iterations is usually less than 50, but it may take more iterations to converge in Algorithm 3. We terminate the outer loop (MM algorithm) when any of the following stopping criteria is satisfied.

1. The change in the value of the objective function, i.e., the negative log likelihood function $-\ell(\mathcal{X}; \Theta)$ is small:

$$|\ell(\mathcal{X}; \Theta^{[m+1]}) - \ell(\mathcal{X}; \Theta^{[m]})| < 10^{-2}$$

or the relative change is small:

$$|\{\ell(\mathcal{X}; \Theta^{[m+1]}) - \ell(\mathcal{X}; \Theta^{[m]})\} / \ell(\mathcal{X}; \Theta^{[m]})| < 10^{-5}.$$

2. The change in factors \mathbf{u}, \mathbf{v} and \mathbf{w} is small:

$$\max\{\|\hat{\mathbf{u}}_\tau^{[m+1]} - \hat{\mathbf{u}}_\tau^{[m]}\|_2, \|\hat{\mathbf{v}}_\tau^{[m+1]} - \hat{\mathbf{v}}_\tau^{[m]}\|_2, \|\hat{\mathbf{w}}_\tau^{[m+1]} - \hat{\mathbf{w}}_\tau^{[m]}\|_2\} \leq 10^{-4}.$$

Based on the general property of MM algorithm (Hunter and Lange, 2004), the objective function value $-\ell(\mathcal{X}; \Theta^{[m]})$ decreases as m gets large and converges to a local minimum of $-\ell(\mathcal{X}; \Theta)$ as $m \rightarrow \infty$. The global and local convergence of our proposed algorithms can be derived similarly as in the work of Zhou et al. (2013) and Wang and Li (2020).

C.3 Clustering Procedure

To avoid local optima, we have extended the clustering procedure from Anandkumar et al. (2014) and Sun et al. (2017) to our problem (2), and suggested to extract R components from L tuples sequentially. We optimize $\ell(\mathcal{X}; \Theta)$ over a rank-one region for L times, and each time we start with either spectral initialization or random initialization. After specifying the number of components R , Algorithm 5 for clustering can identify R components from L estimated tuples of Algorithm 1 by ordering the weights d_τ . To recover the true components $(\mathbf{u}_r^*, \mathbf{v}_r^*, \mathbf{w}_r^*), r \in [R]$, we need to focus on large estimates of d_τ and remove all tuples which are too similar to one another because they will eventually lead to the same component. We terminate the clustering procedure after finding R largest weights, and order the rank-one components according to the magnitude of \hat{d}_j at the end of Algorithm 5. The line 4 of Algorithm 5 is optional, but reestimation with initialization $(\hat{\mathbf{u}}, \hat{\mathbf{v}}, \hat{\mathbf{w}})$ will lead to a more accurate model.

In practice, we could choose the number of initializations, $L = \max\{10, R^3\}$, which works well in most cases. In general, we need large L to avoid local minima for small data sets. The number of initializations L depends on the size of problem (p_1, p_2, p_3, R) and signal-to-noise ratios (SNRs). The clustering procedure will certainly increase the computing time, but it could avoid many local optima for non-convex problems. When the difference between SNRs is smaller, sometimes the order of estimated factor matrices may be flipped when compared with the true factor matrices.

Note that the default threshold ν to remove redundant tuples is set to 0.5 in Algorithm 5, which could be any number between 10^{-4} and 1 as suggested by Sun et al. (2017). This threshold ν is proportional to the size of \mathbf{u}, \mathbf{v} and \mathbf{w} , and small ν will result in more remaining tuples in $S = \{(\hat{d}_\tau, \hat{\mathbf{u}}_\tau, \hat{\mathbf{v}}_\tau, \hat{\mathbf{w}}_\tau), \tau \in [L]\}$. Therefore we should choose ν adaptively depending on the size of data.

Algorithm 5 Clustering Procedure

- 1: **input:** set $S = \{(\hat{d}_\tau, \hat{\mathbf{u}}_\tau, \hat{\mathbf{v}}_\tau, \hat{\mathbf{w}}_\tau), \tau \in [L]\}$.
 - 2: **for** $\tau = 1$ **to** R **do**
 - 3: Find $(\hat{\mathbf{u}}, \hat{\mathbf{v}}, \hat{\mathbf{w}}) = \underset{(\hat{\mathbf{u}}_\tau, \hat{\mathbf{v}}_\tau, \hat{\mathbf{w}}_\tau), \tau \in [L]}{\arg \max} \hat{d}_\tau$.
 - 4: Run Algorithm 1 (3 or 4) with initialization $(\hat{\mathbf{u}}, \hat{\mathbf{v}}, \hat{\mathbf{w}})$ and denote the final update as $(\hat{d}_j, \hat{\mathbf{u}}_j, \hat{\mathbf{v}}_j, \hat{\mathbf{w}}_j), j \in [R]$.
 - 5: Remove all tuples in S with $\min\{\|\hat{\mathbf{u}}_\tau \pm \hat{\mathbf{u}}\|_2, \|\hat{\mathbf{v}}_\tau \pm \hat{\mathbf{v}}\|_2, \|\hat{\mathbf{w}}_\tau \pm \hat{\mathbf{w}}\|_2\} \leq \nu = 0.5, \tau \in [L]$.
 - 6: **end for**
 - 7: **output:** $\{(\hat{d}_j, \hat{\mathbf{u}}_j, \hat{\mathbf{v}}_j, \hat{\mathbf{w}}_j), j \in [R]\}$.
-

D Analysis of Nations Data

D.1 Choice of Rank and Tuning Parameters

In addition to the choice of rank suggested by the marginal explained deviance and weights for the initial unregularized logistic tensor decomposition, we can use the BIC and AIC. As shown in Figure 17, rank $R = 2$ is chosen by BIC criterion, and $R = 4$ is chosen by AIC criterion.

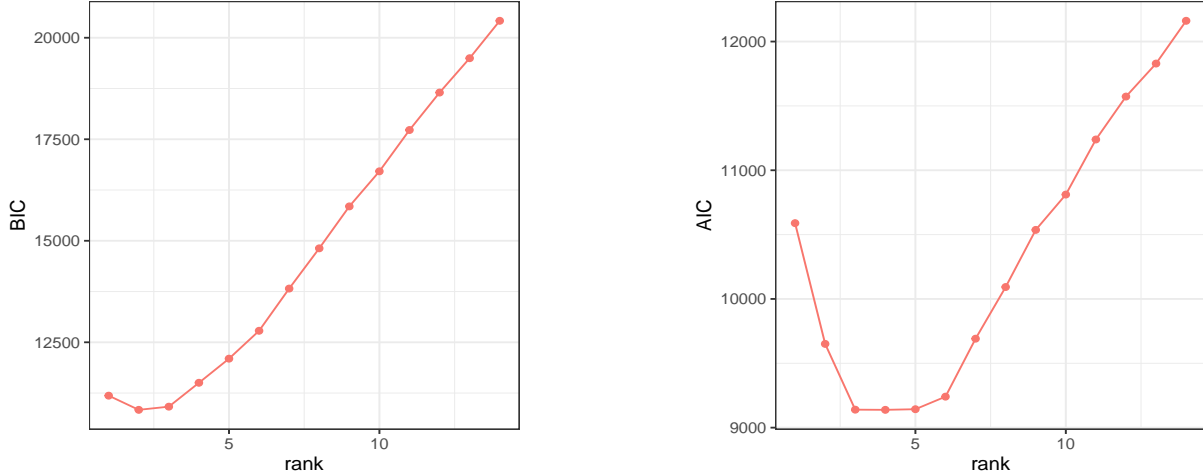


Figure 17: BIC and AIC versus rank R for the nations data.

For the sparse logistic CP decomposition, the estimated offset term μ is -2.86 , and the tuning parameters are chosen by BIC criterion. As shown in Figure 18, four BIC curves versus ratio s suggest 56, 39, 16 and 56 nonzero entries for the first four components respectively.

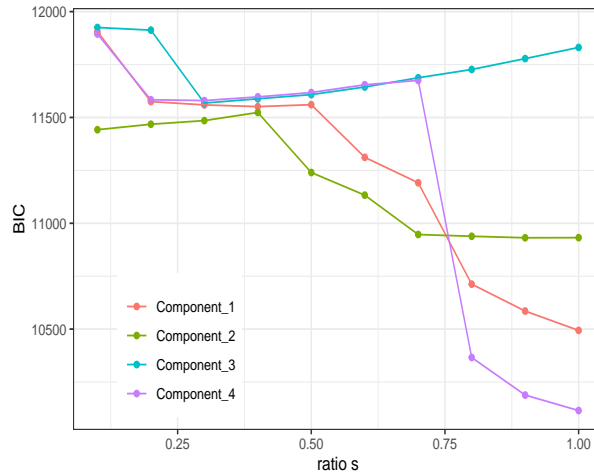


Figure 18: BIC versus ratio s for four relation factors for the nations data.

D.2 Visualization of Components

For component 1 shown in Figure 19, positive values are associated with international partnerships and diplomatic relations. All nations have the same signs, so this component can be viewed as a main effect of relations. For component 2 shown in Figure 20, negative values are associated with hostile actions, zero values are related to exports or population exchanges, and positive values are related to international partnerships. Again, all nations have the same the signs, so this component can be viewed as a main effect of relations. For component 4 shown in Figure 21, negative or hostile actions are on the negative end of the relation factor while international partnerships are on the positive end. The nations can be grouped into two clusters: one with neutral countries and the other with the rest countries. In order to plot the heatmaps using a common scale for visualization,

all entries of the components are divided by the maximum absolute value of all entries and then scaled to between -1 and 1 .

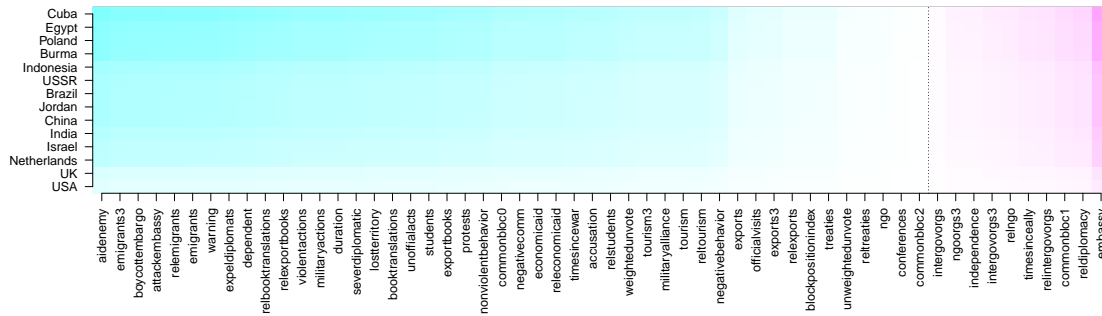


Figure 19: Heatmap of relation versus nation for component 1 with regularization.

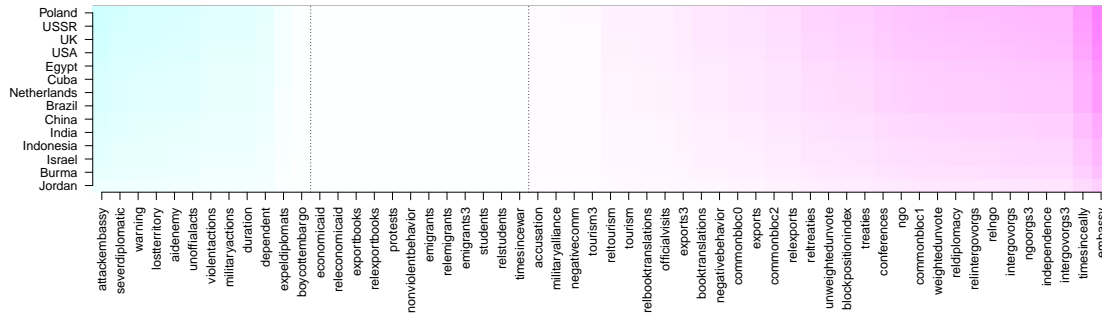


Figure 20: Heatmap of relation versus nation for component 2 with regularization.

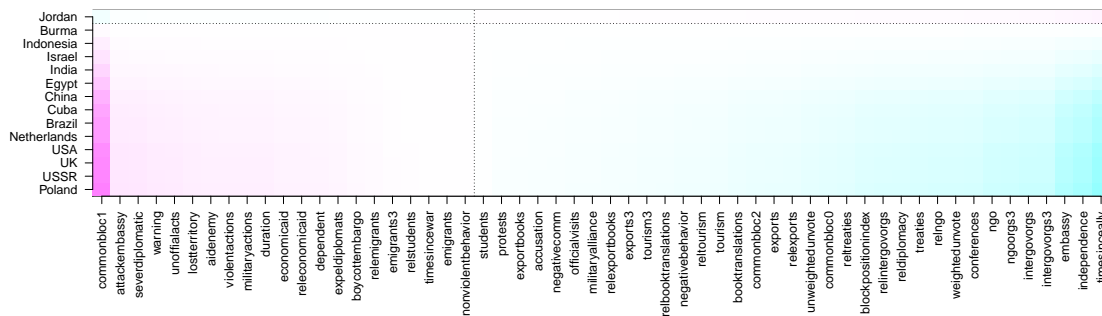


Figure 21: Heatmap of relation versus nation for component 4 with regularization.